IDO-14583

3 2 5
5-22-62

MASTER

CHEMICAL PROCESSING TECHNOLOGY QUARTERLY PROGRESS REPORT October - December, 1961

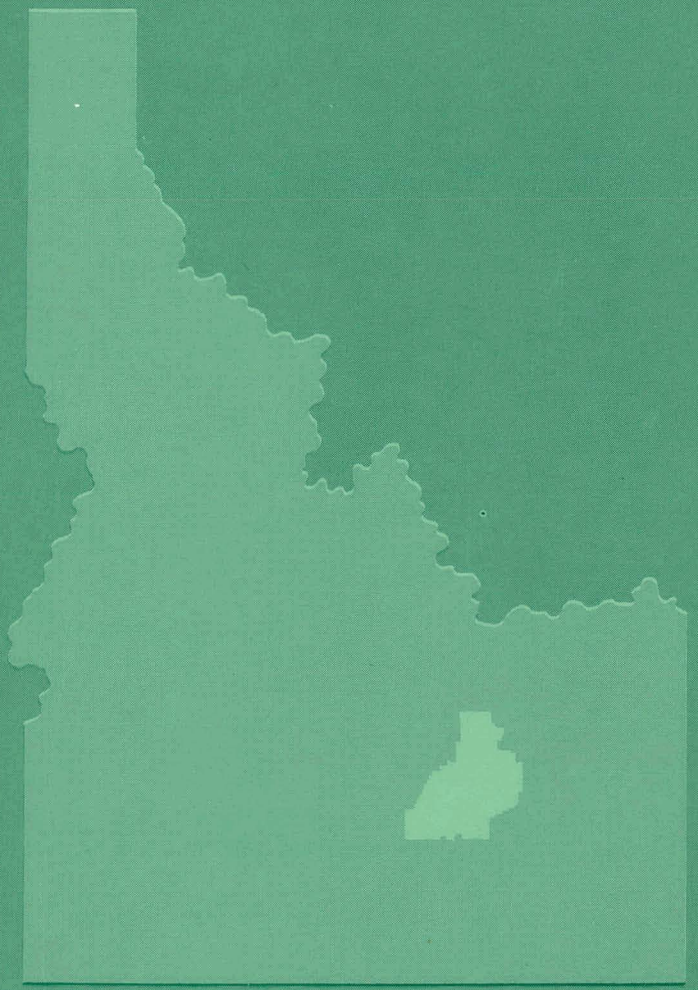

PHILLIPS PETROLEUM COMPANY

ATOMIC ENERGY DIVISION

NATIONAL REACTOR TESTING STATION

US ATOMIC ENERGY COMMISSION

DISCLAIMER

This report was prepared as an account of work sponsored by an agency of the United States Government. Neither the United States Government nor any agency Thereof, nor any of their employees, makes any warranty, express or implied, or assumes any legal liability or responsibility for the accuracy, completeness, or usefulness of any information, apparatus, product, or process disclosed, or represents that its use would not infringe privately owned rights. Reference herein to any specific commercial product, process, or service by trade name, trademark, manufacturer, or otherwise does not necessarily constitute or imply its endorsement, recommendation, or favoring by the United States Government or any agency thereof. The views and opinions of authors expressed herein do not necessarily state or reflect those of the United States Government or any agency thereof.

DISCLAIMER

Portions of this document may be illegible in electronic image products. Images are produced from the best available original document.

PRICE $1.25

Available from the
Office of Technical Services
U. S. Department of Commerce
Washington 25, D. C.

LEGAL NOTICE

This report was prepared as an account of Government sponsored work. Neither the United States, nor the Commission, nor any person acting on behalf of the Commission:

A. Makes any warranty or representation, express or implied, with respect to the accuracy, completeness, or usefulness of the information contained in this report, or that the use of any information, apparatus, method, or process disclosed in this report may not infringe privately owned rights; or

B. Assumes any liabilities with respect to the use of, or for damages resulting from the use of any information, apparatus, method, or process disclosed in this report.

As used in the above, "person acting on behalf of the Commission" includes any employee or contractor of the Commission, or employee of such contractor, to the extent that such employee or contractor of the Commission, or employee of such contractor prepares, disseminates, or provides access to, any information pursuant to his employment or contract with the Commission, or his employment with such contractor.

Printed in USA

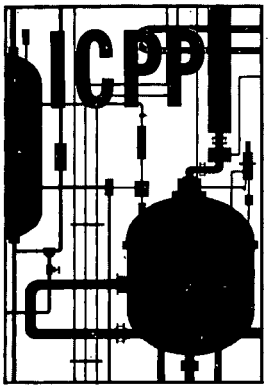

IDAHO CHEMICAL PROCESSING PLANT

IDO-14583
AEC Research & Development Report
General, Miscellaneous, and Progress Reports
TID-4500 (17th Ed.)
Issued: March 28, 1962

CHEMICAL PROCESSING TECHNOLOGY
QUARTERLY PROGRESS REPORT
October - December, 1961

J. R. Huffman
Assistant Manager, Technical

J. A. McBride
Technical Director

J. R. Bower
Editor

PHILLIPS
PETROLEUM
COMPANY

Atomic Energy Division
Contract AT(10-1)-205
Idaho Operations Office
U. S. ATOMIC ENERGY COMMISSION

Previous Quarterly Reports in the ICPP Series

1954

Quarter	Number
2	IDO-14324
3	IDO-14337
4	IDO-14350

1955

Quarter	Number
1	IDO-14354
2	IDO-14362
3	IDO-14364
4	IDO-14383

1956

Quarter	Number
1	IDO-14385
2	IDO-14391
3	IDO-14395
4	IDO-14400

1957

Quarter	Number
1	IDO-14410
2	IDO-14419
3	IDO-14422
4	IDO-14430

1958

Quarter	Number
1	IDO-14443
2	IDO-14453
3	IDO-14457
4	IDO 14467

1959

Quarter	Number
1	IDO-14471
2	IDO-14494
3	IDO-14509
4	IDO-14512

1960

Quarter	Number
1	IDO-14520
2	IDO-14534
3	IDO-14540
4	IDO-14553

1961

Quarter	Number
1	IDO-14560
2	IDO-14567
3	IDO-14574

CHEMICAL PROCESSING TECHNOLOGY
QUARTERLY PROGRESS REPORT
OCTOBER – DECEMBER, 1961

SUMMARY

The ICPP processed aluminum fuel, principally of the MTR-ETR type, during this quarter. Newly designed and installed processing equipment exhibited excellent operating performance. This included direct-air-pulsed extraction, stripping and scrub columns, and a cascade-controlled continuous evaporator in first cycle product concentration service.

Aqueous zirconium fuel processing studies have continued with the objective of adapting the hydrofluoric acid process to continuous dissolution-complexing in order to increase the capacity of the ICPP process while using as much existing equipment as possible to minimize costs. Six variations of hydrofluoric acid flowsheets were tested in small-scale continuous dissolvers. Dissolution rates were found to be high in all cases and dissolution was easily initiated at temperatures as low as 30°C. Monel and Carpenter-20(Cb) were found to be satisfactory construction materials, from the standpoint of corrosion, if oxidizing conditions were carefully controlled. Additional studies are reported on the stability of blended zirconium and aluminum process raffinates and on the nature of the solids which result from the sodium formate headend precipitation process.

Electrolytic dissolution studies, directed at fundamentals of current utilization in a "series"-type dissolver, demonstrated that high current utilization is obtained when the polarization resistance is small compared with the solution resistance. Factors affecting polarization resistance and solution resistance are clarified. A decrease in current utilization observed with alternating current as compared with direct current may be offset by efficiencies in elimination of ac-dc converters required for the dc system. Experimental results indicate the possible usefulness of several plastic and ceramic materials in the chemical and radiation environment of an electrolytic dissolver.

Fluidized bed calcination tests conducted in both pilot plant and Demonstrational Waste Calcination Facility calciners demonstrated that alpha alumina formation was suppressed by addition of boric acid to the waste aluminum nitrate feed. A possible relationship between nozzle design and alpha alumina formation also was noted. Additional laboratory studies on the effect of environmental gas composition on alpha alumina formation were conducted, and pilot plant investigation of calciner off-gas particulate loading demonstrated the effects of nozzle operating conditions on particle attrition.

Pulse column development continued with the goal of specifying and evaluating column control requirements through a study of pulse column dynamics. Use of porous Kel-F and porous stainless steel has provided means of separating and sampling the organic and aqueous phases from the experimental column. Pulse amplitudes in an experimental air pulser were measured by electronic integration of a signal representing the square root of the output of a flow transducer in the pulser leg. Results of calibration runs agree to within five

per cent of the amplitude observed in a glass pulser leg, and, for comparable conditions, to within two to three per cent of values obtained by simulation on an analog computer.

Additional basic process studies reported include an investigation of the distribution of uranium between TBP-Amsco and nitric acid solutions as found in stripping and scrub column conditions and as influenced by the presence of dibutyl phosphate, a TBP degradation product. Other basic studies involve development of a continuous recirculating dissolver, study of the effect of silicon in aluminum alloy fuels on uranium losses, and determination of ion exchange properties and possible usefulness of local natural earth materials in low-level waste treatment.

CHEMICAL PROCESSING TECHNOLOGY
QUARTERLY PROGRESS REPORT
OCTOBER - DECEMBER, 1961

CONTENTS

CONTENTS

CONTENTS

FIGURES

FIGURES

TABLES

I. ICPP OPERATIONAL SCHEDULE, PERFORMANCE, AND PROBLEMS

1. ICPP PROCESSING SCHEDULE
(J. R. Bower, H. E. Stelling)

Idaho Chemical Processing Plant (ICPP) Run No. 19, for the dissolution and recovery of uranium from Materials Testing Reactor-Engineering Test Reactor (MTR-ETR) type fuel elements, was started during this quarter. Some stored recycle and RaLa uranium solutions also were processed. The "blocked-out" method of plant operation was followed, ie, dissolution and first cycle extraction, followed by second and third cycle extraction, using a limited operating crew to carry out the phases in sequence rather than simultaneously. A separate, semi-batch dissolution of Chalk River fuel elements is currently underway.

Dissolution and first cycle extraction varied from about 75 to 100 per cent of the flowsheet rate [1]*. The lower rate, limited by slow dissolution, was for ETR elements. Second and third cycle extraction, limited by column hydraulics, proceeded at about 80 to 90 per cent of the flowsheet rate. The actual flowsheet used was a slight modification of the referenced flowsheet [1] to take advantage of recent equipment modifications. However, publication of the revision does not appear justified, since the changes are small and are still tied to limitations in specific ICPP equipment.

Four barium-140 runs were completed, yielding batches of 18,700 to 27,234 curies of product; recoveries were from 44.1 to 54.9 per cent of theoretical. Total yield was 72,734 curies.

2. ICPP OPERATIONAL PERFORMANCE
(J. R. Bower, H. E. Stelling)

The newly installed first cycle equipment [2] operated satisfactorily and generally exhibited marked improvements in operational characteristics over the originally installed equipment. The direct air pulsers now installed on all pulse-type columns have given excellent performance. Further design information on air pulsed columns is given in a later section (VII) of this report.

Water testing of the new first cycle product evaporator indicated very good performance. A boilup rate of 300 liters per hour was reached, limited by the steam supply system; normal operation calls for a boilup rate of 200 liters per hour. At 300 liters per hour boilup, the over-all heat transfer coefficient was 300 to 350 BTU/(hr)(ft^2)(°F). In actual operation, the new cascade control system has given excellent control of product quality (specific gravity). This is also discussed further in Section VII of this report. The product pumpout to the intermediate storage cell via the new airlift system has been excellent. Line plugging and pump failures encountered with the previous remote head pump system have not occurred.

* Numbers in brackets refer to entries in Section IX, References.

The mixer-settler for contacting the aqueous strip stream with Amsco [3] to remove TBP before concentration, reduced the apparent TBP concentration to 2×10^{-2} grams/liter as compared with the theoretical 3×10^{-3} grams/liter. However, this was at an aqueous-to-organic flow ratio of 20:1 as compared with the flowsheet design of 10:1. The reduced organic ratio was required because of difficulty with the Amsco disposal system, which has been redesigned but not yet rebuilt.

The first cycle "A" column (extraction) continued to exhibit poor interface control and instability. The troubles were attributed in part to surfactant effects of silicon in the feed, poor control of feed rate, and poor performance of the feed cooler. Operation of the column was improved by addition of gelatin to the fuel to give a concentration of 0.05 gram/liter. The ETR fuel being processed was known to contain significant silicon (0.5 weight per cent in the meat, 0.1 wt% in the clad, for over-all composition of 0.3 wt% silicon).

3. PLANT ASSISTANCE PROBLEMS

3.1 High Silicon Alloy Dissolution (H. T. Hahn, Problem Leader; M. R. Bomar)

The behavior of high silicon alloys during dissolution and extraction has not been clearly established. It is conceivable that uranium could be lost to process streams in an insoluble dissolver residue, or be occluded and inextractable from a siliceous product. A brief laboratory investigation of the effect of high silicon content upon uranium losses was initiated late in the quarter. Pieces of silicon-enriched ETR and MTR fuel plates were dissolved by the standard mercury-catalyzed nitric acid procedure.

During dissolution of the ETR plate (8.5 per cent uranium, 0.3 per cent silicon), no insoluble uranium-bearing material appeared other than silica. Washing the silica with 8N nitric acid removed all but 0.03 per cent of the occluded uranium.

The dissolution of the MTR plate (25.6 per cent uranium, 1.3 per cent silicon) did result in some slow-dissolving slivers. The slivers subsequently were identified as pieces of the cladding. The relatively voluminous silicon oxide resulting from this dissolution required more extensive washing with acid to reduce the uranium loss to 0.03 per cent of the original uranium.

It would appear that insoluble intermetallic materials containing significant amounts of uranium are not likely to arise from either type plate. However, it is entirely possible that significant amounts of uranium would be occluded in the silica, since the only washing action available in the IA column is that of tributyl phosphate extraction.

To establish whether tributyl phosphate in Amsco could leach the uranium from the silica as well as the 8N nitric acid used in the above experiments, the residue from an MTR plate dissolution was contacted successively with three 3-1/4 per cent tributyl phosphate-Amsco solutions. The organic extractant was used in a 3:4 volume ratio with the aqueous phase. After the third extraction, the silica residue was found to contain only 0.004 per cent of the original

uranium. It would therefore appear from this single experiment that uranium can be extracted from the silicon in the IA column.

Further work is planned to define the effects of high silicon content upon processing of these alloys.

II. AQUEOUS PROCESS STUDIES

(Section Chiefs: K. L. Rohde, Chemistry; J. I. Stevens, Development Engineering; R. A. McGuire, Development Operations)

1. AQUEOUS ZIRCONIUM FUEL PROCESSING

1.1 Flowsheet Studies on the Continuous Dissolution of Zirconium in Hydrofluoric Acid (D. K. MacQueen, Problem Leader; H. Chamberlain, A. P. Roeh, J. L. Walker, L. J. Moore)

Miniature continuous dissolvers were operated at the Cold Pilot Plant to evaluate several flowsheets for a second generation ICPP headend for zirconium fuels. A continuous version of the present hydrofluoric acid batch dissolution process appears to be the most promising of the potential processes [4]. The major disadvantages of HF dissolution are potentially high dissolver corrosion rates and limited solution stability ranges. A series of small, continuous dissolvers was tested with six possible variations of the HF flowsheet. The two leading contenders for the material of construction, Carpenter-20(Cb) and Monel, were used to fabricate the dissolvers. The primary objective of the tests was the determination of the corrosion characteristics of these flowsheets in Carpenter-20(Cb) or Monel dissolvers. Preliminary process flowsheet data obtained during the course of the tests are reported below. Corrosion data are reported in section 1.2.

1.11 Experimental Equipment and Procedures. A sketch of the test equipment is shown in Figure 1. Construction details of the 1/2-inch pipe

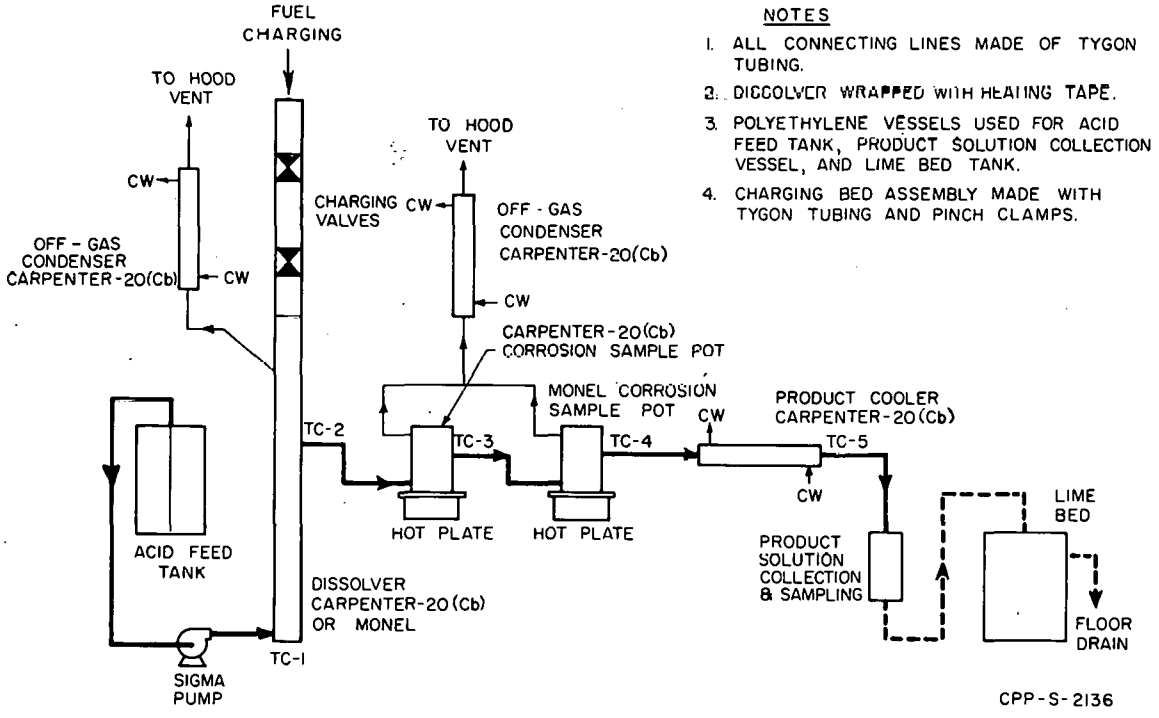

Fig. 1 Miniature zirconium dissolver equipment flow diagram.

dissolvers are shown in Figure 2, and Figure 3 shows the details of the pots holding the corrosion test coupons.

One corrosion test coupon, of the same material as the dissolver, was placed below the fuel-retaining plate in the dissolver. This coupon was used to determine the corrosiveness of incoming acid feed. Three coupons, one each in the vapor, interface, and solution, were tested in each corrosion specimen pot to determine the corrosiveness of the dissolver product solutions. Each coupon was of the same material as the pot. The dissolver bodies were considered as corrosion test specimens for evaluating corrosion during dissolution.

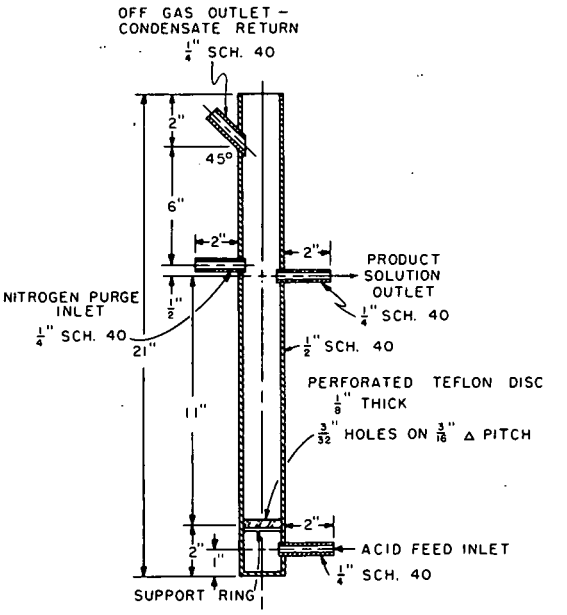

Fig. 2 Miniature zirconium dissolver details.

1.12 Test Results. The nominal compositions of the dissolvents of the six HF process flowsheets tested were:

(1) 10M HF, 0.03M H_2O_2

(2) 10M HF, 0.6M HNO_3

(3) 10M HF, 0.05 M H_2O_2, 0.001M $CuCl_2$, 0.001M $MnCl_2$

(4) 10M HF (aerated)

(5) 4.8M HF, 0.03M HNO_3

(6) 4.2M HF, 0.55M Al $(NO_3)_3$

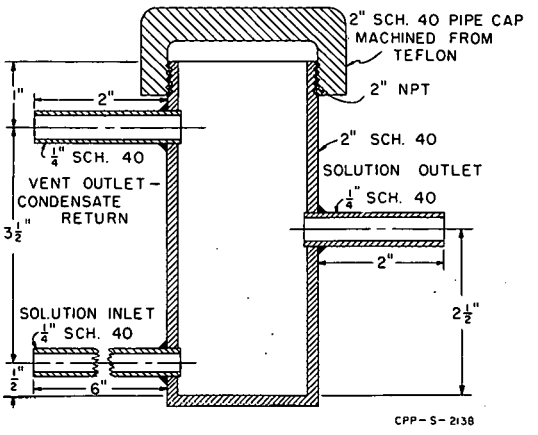

Fig. 3 Corrosion sample pot details.

Operating conditions for the six tests are listed in Table I, and the flowsheet results are shown in Table II. Corrosion results are described in detail in the next section (1.2) of this report.

Some general observations, applicable to all the tests, can be made. Of considerable importance is the observation that 2.1-molar zirconium is the approximate limit of physically stable product solutions. All product solutions less than 2.1-molar zirconium were stable for several seeks; solutions from 2.1 to 2.2 molar were stable for a few days; and solutions over 2.2 molar

Table I

OPERATING CONDITIONS FOR CONTINUOUS ZIRCONIUM DISSOLUTION STUDIES IN MINIATURE DISSOLVERS

Flowsheet No.	Nominal Dissolvent Composition	Dissolver Material	Acid Feed Rate (ml/min)	Dissolution Time		Total Run Time (hr)	Dissolver Operating Temperature
				Zircaloy-2 (hr)	Zircaloy-2 with 1% Uranium (hr)		
1	10.0M HF-0.03M H_2O_2	Carpenter-20(Cb)	6.5	0	188	188	boiling
2	10.0M HF-0.6M HNO_3	Carpenter-20(Cb)	6.5(a)	92.5	0	92.5	boiling
3	10.0M HF-0.05M H_2O_2-0.001M $CuCl_2$-0.001M $MnCl_2$	Monel	7.5	143	46	189	boiling
4	10M HF (aerated)	Carpenter-20(Cb)	7.5	190	0	190	boiling
5	4.8M HF-0.03M HNO_3	Carpenter-20(Cb)	7.5	189	0	189	boiling
6	4.2M HF-0.55M $Al(NO_3)_3$	Carpenter-20(Cb)	7.5	91	48	139	boiling

(a) Feed rate increased to 16 ml/min for several hours without effect on product composition.

Table II

RESULTS OF CONTINUOUS ZIRCONIUM DISSOLUTION STUDIES IN MINIATURE DISSOLVERS

Flowsheet No.(a)	Avg Product Solution Concentration			% Uranium Dissolved(b)	% Oxidation Uranium in solution to hexavalent state(b)	Product Solution Stability			Avg Fluoride to Zirconium Ratio(b)	Solids in Product Solution
	Zr M	H M	Oxidant M			Stable Range Zr M	Metastable Range Zr M	Unstable Range Zr M		
1	0.09	1.01	0.028M H_2O_2	62.1	44.7	< 2.1	2.1 to 2.2	> 2.2	4.90	continuously
2	2.30(c)	0.89	0.45M(d) HNO_3	No U bearing material present	No U bearing material present	No stable solutions produced	2.1 to 2.2	> 2.2	4.50(e) 4.38(f)	continuously
3	2.30(c)	1.65	0.022M H_2O_2	67.3	54.4	No stable solutions produced	No metastable solutions produced	> 2.19	4.90 4.75(g)	continuously
4	2.31(c)	1.46	—	No U bearing material present	No U bearing material present	< 2.1	2.1 to 2.2	> 2.2	4.94(h) 4.56(g)	continuously
5	1.09	0.77	0.032M HNO_3	No U bearing material present	No U bearing material present	0.70 to 1.27	All solutions were stable	All solutions were stable	4.86	continuously
6	0.77	0.64	1.17M HNO_3	103.3	96.4	0.56 to 0.89	All solutions were stable	All solutions were stable	4.92	none

(a) Nominal composition as in Table I.

(b) Based on product solution analyses and uranium charged

(c) Based on total product solution volume and total metal charged during the run. Many of these product solution samples formed a precipitate before analysis.

(d) Average product solution composition at three times the normal flow rate is 2.12M Zr, 0.70M H^+, and 0.43M NO_3^-.

(e) Based on one stable sample.

(f) Based on two samples that formed a precipitate before analysis.

(g) Based on analyses of supernatant solution from samples that formed a precipitate before analysis.

(h) Based on analyses of stable solution samples.

were unstable in the dissolver. Since all four 10-molar HF flowsheets tested produced product solutions 2.1 to 2.3 molar in zirconium, some means of coping with this instability must be a fundamental part of the development program. The solubility diagram is being determined as a function of temperature, time, and F/Zr ratio.

Dissolution rates appeared to be very high. Based on the total fuel content of the dissolvers, the calculated rates ranged from 5.3 to 15.6 mg/(sq cm)(min). The actual rate may have exceeded the calculated rate by an order of magnitude [5] or more, since each time the dissolver was inspected only the fuel pieces at the bottom of the dissolver had been attacked by the dissolvent. It appeared that the HF was reacting almost as soon as it entered the dissolver, and that the net dissolution rate was determined by the quantity of acid added, not by the fuel surface available. This hypothesis was substantiated when only a slight effect on product composition was found upon trebling the feed rate during the tests of flowsheet 2 (see Table I).

1.13 Laboratory-Scale Continuous Dissolution. A dissolver one inch in diameter with a dissolution section 16 inches high has been fabricated from Monel and will be used to obtain process design data on the continuous dissolution of zirconium-uranium alloy fuels using hydrofluoric acid flowsheets. The dissolver and auxiliary equipment have been use-tested, and are ready for operation.

1.2 Corrosion of Carpenter-20(Cb) and Monel During the Continuous Dissolution of Zirconium in Hydrofluoric Acid. (N. D. Stolica, Problem Leader; T. L. Hoffman)

1.21 Preparation of Materials. The dissolver tubes, corrosion pots, and location of corrosion specimens are described in Figures 1, 2, and 3 of the previous section. Similarly, the flowsheets and conditions of operation are summarized in the foregoing section.

The dissolver for the copper- and manganese-catalyzed peroxide flowsheet (No. 3) was made of as-welded Monel; Carpenter-20(Cb) was used for the other five flowsheets. The Carpenter-20(Cb) dissolvers for flowsheet 1 and the first 25-3/4 hours of flowsheet 2 were annealed by soaking the vessels at 2050°F for 15 minutes. The Carpenter-20(Cb) dissolvers for the last 66-3/4 hours of flowsheet 2 and flowsheets 4, 5, and 6 were annealed by soaking the vessels at 2050°F for 45 minutes.

The details of the preparation of the corrosion coupons are included in the tabulated results which follow.

1.22 Results of Evaluation. The detailed results of the corrosion evalutions are given in Tables III through VIII. Each table is discussed briefly and a general conclusion is given at the end of the section.

The data in Table III suggest that both Monel and Carpenter-20(Cb) (with or without heat treatment) are satisfactory materials for vessels handling dissolver product solution from the 10.0 M HF - 0.03 M H_2O_2 flowsheet. However, contact with the dissolver feed at the inlet resulted in deep longitudinal grooves in the Carpenter-20(Cb) dissolver tube and mild general attack on a Carpenter-20(Cb) coupon in contact with the feed solution a short distance away. On the basis of this evidence and Table V, Monel appears to be better suited as a material for the 10.0 M HF - 0.03 M H_2O_2 flowsheet. Carpenter-20(Cb) can be used if it is protected from fresh incoming dissolvent.

The data in Table IV indicate that neither Monel nor Carpenter-20(Cb) is suitable for handling the 10.0 M HF - 0.60 M HNO_3 flowsheet, although Monel was somewhat more resistant to the dissolver product solution than was Carpenter-20(Cb). The Carpenter-20(Cb) corrosion pot suffered a nozzle failure in 68.5 hours, which was equivalent to a corrosion rate of 0.72 ipm; the dissolver tubes showed as great or a greater rate of attack. Carpenter-20(Cb) suffered catastrophic attack in the dissolver feed solution. No data were obtained with Monel in dissolver solution; however, Monel probably would not be fully satisfactory in this service.

Table V lists the corrosion resistance of the alloys for the 10.0 M HF - 0.03 M H_2O_2 flowsheet containing 0.001 M $CuCl_2$ and 0.001 M $MnCl_2$. Service test observations indicate that both annealed Carpenter-20(Cb) and as-welded Monel are suitable for this flowsheet over 189 hours. The Mn^{++} and Cu^{++} salts

Table III

CORROSION OF MONEL AND CARPENTER-20(Cb)
DURING DISSOLUTION OF ZIRCONIUM-URANIUM FUEL IN FLOWSHEET 1

0.03 M H_2O_2 - 10.0 M HF Dissolvent - 188 hr Exposure				
Alloy and Test Sample	Environment	Specimen Treatment	Temperature of Exposure (°F)	Corrosion Rate (ipm)
Monel	Diss. Product			
coupons	liquid	As-received, unwelded & machined	180-200	0.0005
coupons	liquid		180-200	0.0007
coupons	vapor		180-200	0.0008
coupons	vapor		180-200	0.0011
pot	liq.-vapor		180-200	resistant
Carpenter-20(Cb)	Diss. Product			
coupons	liq.-vapor	As-welded, machined & sensitized	180-200	0.0002
coupons	liquid		180-200	0.0002
coupons	liquid	Unwelded, machined & annealed	180-200	0.0002
coupons	liquid		180-200	0.0002
coupons	vapor		180-200	0.0003
coupons	vapor	1250°F sensitized	180-200	0.0003
pot	liq.-vapor	2050°F annealed	180-200	resistant
coupons	Diss. Feed	Unwelded, machined & 1250°F sensitized	100-115	0.0041
Dissolver Tube	Diss. Feed & Diss. Product	15 min annealed 2050°F	100-115	Localized attack deep groves

were added in an effort to catalyze the peroxide oxidation of U(IV) to U(VI); part of the uranium remained in the $^{+4}$ state in these experiments.

Table VI suggests that both Carpenter-20(Cb) and Monel can be used in aerated 10-molar HF flowsheet service, with or without subjecting the Carpenter-20(Cb) to a heat treatment. At temperatures below 160°F, Carpenter-20(Cb) suffered only mild corrosion in the incoming dissolver feed solution. At a somewhat higher temperature (190°F), the alloy also resisted the dissolver product solution during the 189-hour exposure. At temperature of 180 to 190°F, Monel coupons which were immersed in this product solution and the product solution vapors suffered about 0.03 mil and 10.0 mils corrosion per month, respectively.

The 4.8 M HF - 0.03 M HNO_3 - 1.09 M Zr dissolver product solution (Table VII) from the "dilute flowsheet" corrodes Carpenter-20(Cb), but is less corrosive to Monel. The vapors corrode Monel, but are less corrosive to Carpenter-20(Cb). Variations in heat treatment of Carpenter-20(Cb) failed to produce measureable differences in the corrosion rate. For limited service -- up to at least 189 hours -- either of the alloys tested appears satisfactory. Data from Table VII generally suggest that Carpenter-20(Cb) is the preferred

Table IV

CORROSION OF MONEL AND CARPENTER-20(Cb)
DURING DISSOLUTION OF ZIRCONIUM ALLOY IN FLOWSHEET 2

Alloy and Test Sample	Environment	Specimen Treatment	Temperature of Exposure (°F)	Corrosion Rate (ipm)
0.60 M HNO_3 - 10.0 M HF Dissolvent - 92.5 hr Exposure				
Monel	Diss. Product			
coupons	liquid	As-received, welded & machined	140-190	0.0158
coupons	liquid		140-190	0.0208
coupons	vapor		140-190	0.0067
coupons	vapor		140-190	0.0056
pot	liq.-vapor		140-190	resistant
Carpenter-20(Cb)	Diss. Product			
coupons	liq.-vapor	As-welded, machined & 1250°F sensitized	140-190	0.0527
coupons	liquid		140-190	0.0835
coupons	liquid	Unwelded, machined & 2050°F annealed	140-190	0.0727
coupons	liquid		140-190	0.0717
coupons	vapor		140-190	0.0130
coupons	vapor	1250°F sensitized	140-190	0.0130
pot	liq.-vapor	2050°F annealed	140-190	failure(a)
coupons	Diss. Feed	Unwelded, machined, & 1250°F sensitized	100-150	0.3347
Dissolver Tube	Diss. Feed Diss. Product	2050°F, 45 min annealed	100-150	1.18(b)

(a) Nozzle failure 68.5 hr, 0.7200; also general attack of pot.

(b) Represents complete penetration of tube in 66.8 hr for flowsheet using 0.60 M HNO_3. Two other tubes suffered complete penetration in 2.5 and 23 hr, respectively, using the same flowsheet with slightly different HNO_3 concentrations.

material. However, a reduction of the observed corrosion rate associated with the Monel in the dissolver product solution vapors might be achieved by operation under air-free vapor conditions.

Monel was unsatisfactory in the 4.2 M HF - 0.55 M $Al(NO_3)_3$ flowsheet, failing completely (Table VIII). The presence of weld stress cracks in the Carpenter-20(Cb) dissolver tube indicates that this alloy also would be unsatisfactory for extended use with the aluminum nitrate-hydrofluoric acid flowsheet. Since the dissolver had been carefully annealed, the risk of using Carpenter-20(Cb) under these conditions is emphasized.

Table V

CORROSION OF MONEL AND CARPENTER-20(Cb)
DURING DISSOLUTION OF ZIRCONIUM-URANIUM FUEL IN FLOWSHEET 3

0.03 M H_2O_2 - 10.0 M HF Dissolvent Catalyzed with $CuCl_2$ and $MnCl_2$
189 hr Exposure

Alloy and Type Sample	Environment	Specimen Treatment	Temperature of Exposure (°F)	Corrosion Rate (ipm)
Monel	Diss. Feed			
coupons	liquid	As-received, unwelded & machined	110-180 usually 130-150	0.0072
dissolver tube	Diss. Feed Diss. Product	As-welded	110-180	resistant(a)
pot	Diss. Product liq.-vapor	As-welded	150-200 usually 170-190	resistant
Carpenter-20(Cb)	Diss. Product			
pot	liq.-vapor	2050°F annealed	150-200 usually 170-190	resistant

(a) Fuel plate support rings underwent aggressive attack. These rings were fabricated from Monel weld wire and do not have the same composition as wrought Monel (dissolver and coupons).

1.23 Conclusions of Corrosion Studies. These experiments indicated, in general, that Monel and Carpenter-20 were suitable for service in 10-molar hydrofluoric acid even under mild oxidizing conditions as with dilute hydrogen peroxide. Neither material would be suitable for long-term use with the more concentrated oxidant solutions. Monel may be preferred over Carpenter-20 because of the possibility that the latter may not be adequately annealed in the field and may fail at sensitized areas in or adjacent to welds, whereas Monel can be satisfactorily field-welded.

Table VI

CORROSION OF MONEL AND CARPENTER-20(Cb)
DURING DISSOLUTION OF ZIRCALOY-2 IN FLOWSHEET 4

Aerated 10 M HF Dissolvent - 189 hr Exposure				
Alloy and Type Sample	Environment	Specimen Treatment	Temperature of Exposure (°F)	Corrosion Rate (ipm)
Monel	Diss. Product			
coupons	liquid	As-received, unwelded & machined	180-190	0.0003
coupons	liquid		180-190	0.0003
coupons	vapor		180-190	0.0079
coupons	vapor		180-190	0.0093
pot	liq.-vapor		180-190	resistant
Carpenter-20(Cb)	Diss. Product			
coupons	liq.-vapor	As-welded, machined & sensitized	180-190	0.0007
coupons	liquid		180-190	0.0002
coupons	liquid	Unwelded, machined & 2050°F annealed	180-190	0.0001
coupons	liquid		180-190	0.0003
coupons	vapor		180-190	0.0006
coupons	vapor	1250°F sensitized	180-190	0.0007
pot	liq.-vapor	2050°F annealed	180-190	resistant
coupons	Diss. Feed	Unwelded, machined & 1250°F sensitized	90-160 usually 140-160	0.0002
dissolver tube	Diss. Feed Diss. Product	2050°F, 45 min annealed	90-160 usually 140-160	resistant

Table VII

CORROSION OF MONEL AND CARPENTER-20(Cb)
DURING DISSOLUTION OF ZIRCALOY-2 IN FLOWSHEET 5

Alloy and Type Sample	Environment	Specimen Treatment	Temperature of Exposure (°F)	Corrosion Rate (ipm)
0.03 M HNO_3 - 4.8 M HF Dissolvent - 189 hr Exposure				
Monel	Diss. Product			
coupons	liquid	As-received, unwelded & machined	180-200	0.0013
coupons	liquid		180-200	0.0013
coupons	vapor		180-200	0.0053
pot	liq.-vapor		180-200	resistant
Carpenter-20(Cb)	Diss. Product			
coupons	vapor-liq.	As-welded, machined & 1250°F sensitized	180-200	0.0008
coupons	liquid		180-200	0.0028
coupons	liquid	Unwelded, machined & 2050°F annealed	180-200	0.0024
coupons	liquid		180-200	0.0025
coupons	vapor		180-200	0.0008
coupons	vapor	1250°F sensitized	180-200	0.0007
pot	liq.-vapor	2050°F annealed	180-200	resistant
dissolver tube	Diss. Feed Diss. Product	2050°F, 45 min annealed	90-130 mostly 100	resistant

Table VIII

CORROSION OF MONEL AND CARPENTER-20(Cb)
DURING DISSOLUTION OF ZIRCONIUM-URANIUM FUEL IN FLOWSHEET 6

Alloy and Test Sample	Environment	Specimen Treatment	Temperature of Exposure (°F)	Corrosion Rate (ipm)
0.55 M $Al(NO_3)_3$ - 4.2 M HF Dissolvent - 139 hr Exposure				
Carpenter-20(Cb)	Diss. Feed			
coupons	liquid	1250°F sensitized	90-150 usually 110-130	0.0074
dissolver	Diss. Feed Diss. Product	2050°F, 45 min annealed	90-150 usually 110-130	weld stress cracks
pot	Diss. Feed Diss. Product	2050°F, 45 min annealed	180-200	resistant(a)
Monel	Diss. Product			
pot	liq.-vapor	as-welded	180-200	0.7992

(a) Fuel plate support rings underwent aggressive attack. These rings were fabricated from Carpenter-20(Cb) weld wire and do not have the same composition as wrought or weld-deposited (cast) Carpenter-20(Cb).

1.3 Dissolution Kinetics of Zircaloy-Uranium Fuel in Hydrofluoric Acid (D. W. Rhodes, Problem Leader; B. J. Newby)

Scoping experiments were made to determine the minimum temperature necessary to initiate and sustain a reaction between Zircaloy-2 or Zircaloy-2 1-1/2 per cent uranium fuel and the feed and dissolver product of the "dilute" (4.8 M HF) and "slurry" (10 M HF) flowsheets. The "dilute" flowsheet is described by Parrett [4], and the "slurry" flowsheet is identical to the continuous STR flowsheets 1, 2, and 3 described by Parrett [4] except that no oxidant is used in the dissolver, thus leaving part of the uranium and all of the tin as solids.

1.31 Experimental Procedure. The experiments were performed by stirring a convenient weight of fuel with 25 milliliters of solution at the appropriate temperature. Dissolution rates usually were obtained by determining the weight loss of a fuel piece after 5 minutes' dissolution; a 30-minute period was used for rates 0.1 mg/(cm^2)(min) or lower, and a 1-minute period was used for rates above 100 mg/(cm^2)(min).

1.32 Experimental Results. The results of these experiments are summarized in Table IX. All temperatures refer to temperature prior to dissolution. The temperature increased as the dissolution proceeded.

The results listed in Table IX indicate that the dissolution of zirconium-containing fuel in dissolver feed containing hydrofluoric acid can be initiated and sustained at 30°C or higher under "dilute" or "slurry" flowsheet conditions.

1.33 Dissolution of Solids in Dissolver Product. Dissolver product solution containing undissolved uranium tetrafluoride and tin was obtained by dissolving 1-1/2 per cent uranium - Zircaloy-2 fuel under "slurry" flowsheet

Table IX

DISSOLUTION OF ZIRCONIUM FUEL

Fuel	Dissolver Solution	Initial Temperature (°C)	Approximate Dissolution Rates (mg cm^{-2} min^{-1})
Unoxidized Zr-2	slurry flowsheet product	19	barely visible reaction
Unoxidized Zr-2	slurry flowsheet product	30	9
Unoxidized Zr-2	dilute flowsheet product	23	0.8
Unoxidized Zr-2	dilute flowsheet product	30	1.4
Oxidized Zr-2	slurry flowsheet product	24	no reaction
Oxidized Zr-2	slurry flowsheet product	30	0.1
Oxidized Zr-2	dilute flowsheet product	23	no reaction
Oxidized Zr-2	dilute flowsheet product	30	barely visible reaction
Oxidized Zr-2	10 M hydrofluoric acid	30	200
Oxidized Zr-2	4.8 M hydrofluoric acid	30	2.8
1.5% U-Zr-2	slurry flowsheet product	19	barely visible reaction
1.5% U-Zr-2	dilute flowsheet product	23	0.8

conditions. The tin and uranium dissolved within one minute at 25°C when two volumes of dissolver product were mixed with three volumes of a solution containing 0.9-molar aluminum, 0.8-molar hydrogen ion, 0.4-molar fluoride, 0.028-molar chromic acid, and 3.2-molar nitrate (coarse feed adjustment solution for the "slurry" flowsheet).

1.4 Blending Raffinates from Zirconium and Aluminum Processes (D. W. Rhodes, Problem Leader; B. J. Newby)

The blending of zirconium and aluminum fuel raffinates to reduce corrosion and make additional tank storage available for the zirconium raffinates is being investigated on a laboratory scale. This investigation consists of storing the raffinates blended in various proportions [3] at 35 and 55°C. Periodic observations have been made for 17 weeks to determine the stability of the blended raffinates. All blends stored at 55°C were unstable, ie, solids formed. At 35°C, all blends containing 30 per cent by volume or less zirconium raffinate were stable, and a few blends containing higher concentrations of zirconium raffinate also were stable. The volume of settled residue in the unstable samples varied from a trace to about 16 per cent of the total volume.

Solids from six of the most unstable blends at 55°C were examined by X-ray diffraction. One solid could not be identified; the other five solids were determined by X-ray diffraction to contain the crystalline compound Zr_2OF_6 or $Zr(OH)F_3$, a compound prepared and identified in earlier studies at the ICPP [6].

1.5 Fluozirconate Precipitation Process (D. W. Rhodes, Problem Leader; B. J. Newby)

That addition of sodium formate to hydrofluoric acid-zirconium fluoride dissolver product solutions precipitates the zirconium and fluoride almost quantitatively has been reported previously [7]. This precipitation, which can be made part of a headend operation to remove the alloy metals and fluoride from the process solution prior to purification and recovery of the uranium by solvent extraction, has been under study for some months.

Identification of the zirconium fluoride precipitate was attempted by classical analytical methods and X-ray diffraction. The precipitate (washed free of excess reagents) contained about 1.5 moles of sodium and 5 moles of fluoride for each mole of zirconium. No organic radical (formate) was present. An X-ray diffraction pattern of the major crystalline species was similar to the pattern for βNa_2ZrF_6, but positive identification was not possible. Thus, the precipitate appears to be a mixture composed of sodium fluozirconate salts and, very likely, hydrolysis products of these salts.

III. ELECTROLYTIC DISSOLUTION SYSTEMS
(Section Head: K. L. Rohde)

1. ELECTROCHEMISTRY OF NICHROME IN NITRATE SOLUTIONS
(J. R. Aylward, E. M. Whitener)

A topical report [8] on the electrolytic dissolution of Nichrome in nitrate solutions has been completed. The pertinent conclusions are summarized as follows:

(a) The potential-current density curves follow the Tafel equation ($\eta = a + b \log I$) where the slope (b) is equal to 0.038 volt for all the solutions and temperatures studied. In the Tafel region, the current density at constant potential is independent of hydrogen ion concentration, but does depend on nitrate ion concentration. The dissolution rate at constant potential increases as the nitrate ion concentration is decreased. In this region, the energy of activation for dissolution is 13.2 Kcal/mole.

(b) In some cases, a limiting current density due to concentration polarization is observed at current densities greater than 0.1 amp/cm^2; this limiting current density also increases as the nitrate ion and Nichrome cation concentrations decrease. However, in a typical dissolver solution containing 116 g/l nickel and chromium in the 20-80 Nichrome weight ratio, at 70°C, concentration polarization is absent up to 4 amp/cm^2. Operating temperatures between 70 and 80°C are recommended.

(c) In the limiting current density region, the reaction rate is controlled by the mass transport of reaction products away from the metal-solution interface. Therefore, the dissolution rate can be increased by agitation, higher temperature, and the use of solutions in which nickel and chromium nitrates have a higher solubility (low excess nitric acid). It is concluded that an operating temperature of 70°C is sufficient to eliminate concentration polarization, provided the nitric acid concentration is less than 10 molar.

2. ELECTROLYTIC DISSOLUTION OF ZIRCONIUM IN HYDROCHLORIC ACID-METHANOL
(H. T. Hahn, J. R. Aylward and E. M. Whitener)

A topical report [9] pertaining to the electrochemistry and process implications of electrolytic dissolution of zirconium in hydrochloric acid-methanol has been completed. The results of this investigation may be summarized as follows:

(a) At low overvoltage values, both the anodic and cathodic reactions are activation-controlled. The reaction rates in this region are independent of hydrochloric acid concentration.

(b) Dissolution in the overvoltage range 0 to +0.4 volt is accompanied by the separation of finely divided alpha-zirconium from the electrode. The

amount of residue decreases with increasing overvoltage, with no residue formed at high anodic overvoltages.

(c) At high anodic overvoltages where complete dissolution is attained, the current density is independent of potential. This limiting current density decreases with increasing hydrogen chloride concentration, and here the rate is controlled by mass transport.

(d) The energy of activation for the corrosion reaction (0.0 volt), is 16.5 Kcal/mole; the electropolishing reaction (1.0 volt) has an activation energy of 7.7 Kcal/mole.

(e) The data support the hypothesis that in the activation-controlled region the rate-determining step is electron transfer. In the electropolishing region, the controlling step is the dissolution of a film, possibly $ZrCl_4$.

(f) The rate of dissolution or current density for a zirconium electrode in HCl-methanol solution is given below:

$$I = \frac{\exp\left[20.09 - \frac{8294}{T} + \frac{\eta}{5.03 \times 10^{-4}T - 0.0988}\right] - \exp\left[20.09 - \frac{(8294 + 4350)}{T}\right]}{1 + C^{0.469} \exp\left[6.07 - \frac{4430}{T} + \frac{\eta}{5.03 \times 10^{-4}T - 0.0988}\right]}$$

where η = overvoltage (-0.5 to + 2.0 volts)

T = temperature (273 to 323°K)

C = HCl concentration (1.5 to 13 M).

(g) In limited tests, stainless steel, iron, nickel, and chromium were found to dissolve electrolytically, while aluminum and uranium dissolved chemically, in HCl-methanol at feasible rates and with no evidence of solids formation.

3. SERIES DISSOLVER DEVELOPMENT
(H. T. Hahn, Problem Leader)

The "series" electrolytic dissolver concept [10] was investigated from a fundamental point of view to determine the factors affecting the current utilization. From this study it was hoped to establish the feasibility and design criteria of a practical "series" electrolytic dissolver for nuclear fuel elements.

3.1 Rigorous Mathematical Approach (D. P. Pearson)

An attempt was made to derive an equation relating the current density on a dissolving fuel piece to the cell and fuel piece geometries, solution conductance, total voltage, total current, and the electrochemical properties of the fuel material (reversible potential, limiting current density, and Tafel slope). Generalized geometrical models lead to differential equations which

are believed to be insoluble. In the absence of polarization, mathematical solutions exist for very simple geometries. The effect of polarization may be added as a perturbation to give approximate general solutions. Then, the solutions for simple geometries may be combined to give solutions for more complex geometries. The calculations involved in the last two steps are simple but rather lengthy, and a computer should be used for routine calculations. The geometrical limitations on the models which can be studied in this way may be too severe, and therefore the following simplified approach was adopted.

3.2 Simplified Approach (M. R. Bomar, J. R. Aylward)

A highly simplified approach was made, in which the solution and the dissolving metal were considered as two independent resistances in parallel. The following equation was derived in terms of the percentage current utilization per piece, U, the solution resistance, R_S, and the polarization resistance, R_p.

$$\frac{100}{U} = 1 + \frac{R_p}{R_s} \qquad (1)$$

The percentage current utilization, U, is given by $U = 100\ I_p\ (I_p + I_S)$, where I_p and I_S represent the current passing through the metal and the solution, respectively.

The solution resistance, R_S, is given by

$$R_s = K\ \frac{L}{A} \qquad (2)$$

where K is the specific resistance, A the cross section area of the solution, and L the length of the dissolving piece in the direction of the current flow.

Substitution of Equation (2) into Equation (1) gives

$$\frac{100}{U} = 1 + \left[\frac{R_p A}{K}\right] \frac{1}{L} \qquad (3)$$

so that a plot of 100/U versus 1/L at constant current should give a straight line of slope $\frac{R_p A}{K}$

The polarization resistance, R_p, is a function of current density and in the simplest case (Tafel relationship),

$$R = aI^{-\alpha} \qquad (4)$$

where a and α are constants. When there is secondary passivation or a limiting current density, the function is more complex. Some examples of the latter cases are shown in Figure 4, where the resistance for the anodic part of the electrode reaction is plotted as a function of current density. When alternating current is used for dissolution, the double layer capacity also must be taken into account. The simplest way to represent this is with a capacitor in parallel with the polarization resistance. This capacitor represents an alternate current path so that the current utilization will be less with alternating

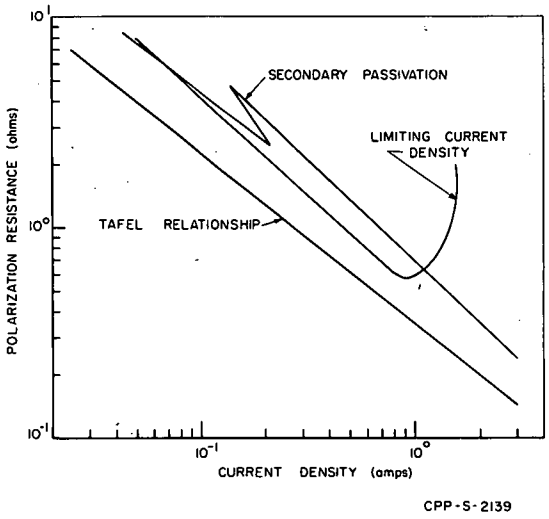

Fig. 4 Selected examples of polarization resistance as a function of current density.

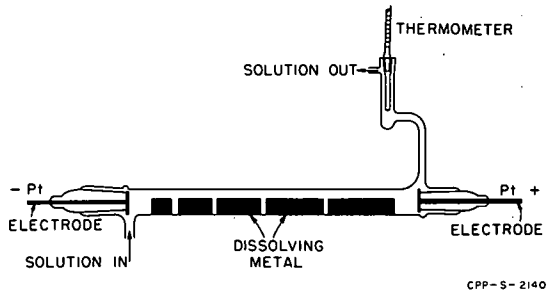

Fig. 5 Series electrolytic dissolver cell.

current than direct current. Also, higher frequencies will result in lower current utilization.

Experiments on the "series" dissolver were carried out in the cell shown in Figure 5. The inside diameter of the cell was 20 millimeters and the distance between the inert platinum electrodes was 300 millimeters. Five pieces of 304 stainless steel, 12.7 millimeters in diameter and of various lengths ranging from 20 to 100 millimeters, were placed in the cell. These pieces were separated from each other by a distance of approximately 6.5 millimeters. A few runs were also made with pieces 6.4 millimeters in diameter. A solution containing 1.2-molar nitric acid plus 4.2-molar nitrates of Fe^{+3}, Ni^{+2} and Cr^{+3} was circulated from a reservoir through the cell at a rate sufficient to maintain the temperature at 50°C. Experiments were conducted at different currents with both dc and ac (60-cycle). The amount of material dissolved from each piece was determined by weight loss and compared with the number of coulombs passed through the cell.

Some results of these experiments are shown in Figure 6 in which 100/U is plotted versus 1/L. From this it can be seen that the current utilization, U, decreases with decreasing current and piece length. This is due to increasing polarization resistance (see Figure 4) and decreasing solution path resistance, respectively. The current utilization is also much lower with 60-cycle ac because of the low frequency response of the electrochemical systems due to the double layer capacitance and passivation phenomena.

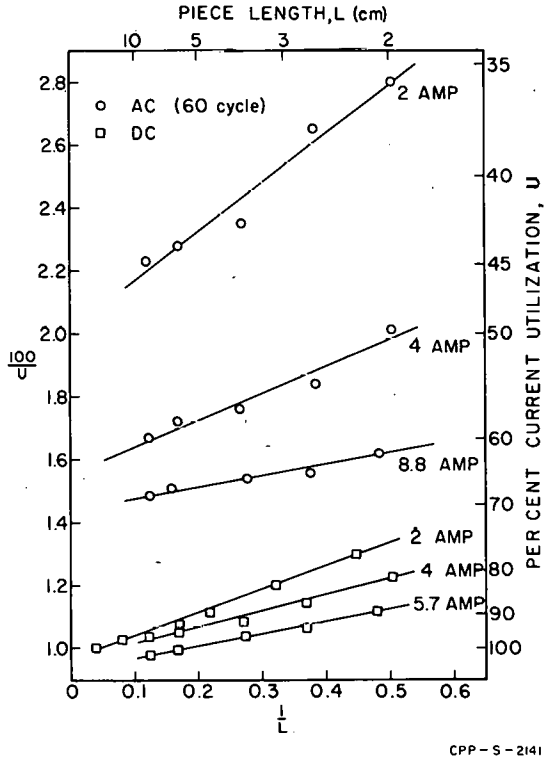

Fig. 6 Effect of piece length and current on current utilization per piece in series dissolution.

The use of smaller-diameter pieces will result in an increase in the polarization resistance, R_p, and the cross sectional area, A, of the solution. The slope, $\frac{R_p A}{K}$, of a 100/U versus 1/L plot will, therefore, increase with decreasing piece diameter. Experimental verification of this is shown in Figure 7.

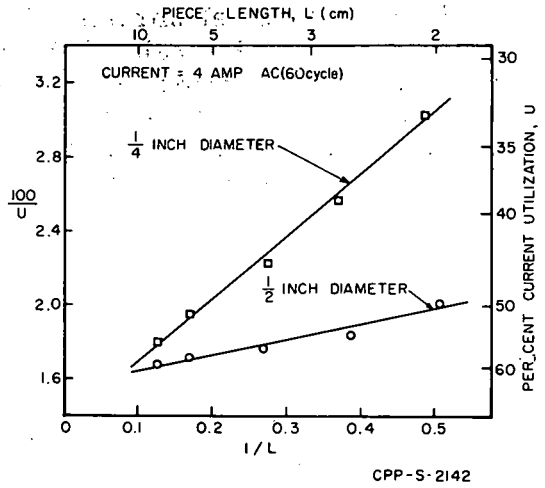

Fig. 7 Effect of piece diameter on current utilization per piece.

3.3 Conclusions

It has been shown that for a "series"-type electrolytic dissolver, high current utilization is obtained when the polarization resistance is small compared to the solution path resistance. Polarization resistance, in general, decreases with increasing current density, while the solution resistance increases with increasing piece length and decreasing solution cross sectional area. Although a decrease in current utilization is observed with alternating current, the effect may be offset by the elimination of ac to dc converters in an electrolytic plant. In a practical "series" dissolver where some of the pieces are in contact, the current utilization is decreased because of the shorting out of the individual cells. However, some of the pieces may be kept insulated from each other by oxide films or residues.

4. MATERIALS OF CONSTRUCTION IN ELECTROLYTIC SYSTEMS

(R. D. Fletcher, Problem Leader; L. A. Decker)

Exploratory and confirmatory tests on candidate insulating materials for the electrolytic dissolver were continued.

4.1 Preliminary Chemical Tests

G-7, a glass fabric-silicone resin sample furnished by Taylor Fiber Co., was tested in electrolytic dissolver product, 1 M HNO_3 - 75 g/l stainless-steel components, at the boiling point for 96 hours. The laminate was unchanged except for a slight loss of color.

Campco S 109, a polystyrene supplied by the Campco division of Chicago Molded Products, also was tested in the dissolver product solution at the boiling point. The samples were completely disintegrated after 48 hours.

4.2 Irradiation Tests

Samples of G-7 laminate (Taylor Fiber Co.), polypropylene (Nalge Co.), annealed Kynar (Pennsalt Co.), and polystyrene (Styron 475-6034, Auburn Plastics Co.), were irradiated at an average dose rate of 4.07×10^6 roentgens to a total dose of 1×10^8 roentgens in boiling dissolver product (1 M HNO_3,

1.5 M stainless-steel nitrates). Samples of G-7 laminate (Taylor Fiber Co.), annealed Kynar (Pennsalt Co.), 96 per cent alumina (McDanel Refractory Porcelain Co.), and 99 per cent alumina (McDanel Porcelain) were also irradiated in the same environment to a total dose of 1×10^9 roentgens. All samples had passed earlier preliminary chemical screening tests. Visible changes in the irradiated samples are recorded in Table X.

Table X

VISIBLE CHANGES IN PLASTIC AND CERAMIC SAMPLES AFTER GAMMA IRRADIATION

Material	Appearance after Irradiation at: 1×10^8R	1×10^9R
G-7	slight color change no obvious damage	slight color change no obvious damage
Polypropylene	slight color change internal cracks	—
Polystyrene (Styron)	warped - stiffer	—
Annealed Kynar	slight color change no obvious damage	slight color change no obvious damage
96% Alumina	—	slight color change no obvious damage
99% Alumina	—	slight color change no obvious damage

Conditions: Contact with 1 M acid, 75 g/l stainless-steel components at 214°F.

IV. NEW WASTE TREATMENT METHODS
(Section Chief: K. L. Rohde, Chemistry)

1. DISPOSAL OF LOW-LEVEL RADIOACTIVE WASTES
(D. W. Rhodes, Problem Leader; M. W. Wilding)

A preliminary laboratory investigation* was conducted on the use of available natural earth materials as potential ion exchangers for the removal of radioisotopes from low-level radioactive wastes at the National Reactor Testing Station. The per cent ash, per cent carbonate, and exchange capacities of a wide variety of earth materials from southeastern Idaho were determined. The carbonate content varied from 0.8 to 18.1 per cent by weight for 14 different materials. Thirteen of these materials had an ash content, on ignition to 1000°C, of greater than 73 per cent by weight, indicating the predominance of non-volatile inorganic material; the ash content of one material was only 12.7 per cent, indicating that the sample was largely organic. The cation exchange capacities varied from 0.05 to 0.76 milliequivalent per gram of solid, but did not appear to be directly related to either the carbonate or ash content of the earth materials.

Batch equilibrium-type experiments were completed with six of the materials to determine their ability to remove cesium and strontium from aqueous solutions. The maximum removal of strontium (1.0 mg/liter, 23°C) occurred at approximately pH 9.0. Maximum distribution coefficients (g Sr per g solid/g Sr per ml solution) at this pH were about 1000 for all six materials. The effect of phosphate on the adsorption of strontium by a calcareous material (13 per cent carbonate) was studied by adding a solution containing 0.1-molar phosphate as di-sodium phosphate. The intent was to determine if phosphate could increase the distribution coefficient for strontium in a calcareous soil through a calcite-phosphate type reaction. The distribution coefficient for strontium was increased throughout the pH range studied (pH 5-10), with a five-fold increase at pH 10. The maximum removal of cesium (1.0 mg/liter, 23°C) by the same earth materials occurred in the slightly acid region (approximately pH 6.0). Materials exhibiting the highest potential for removing fission products from solution and having the best physical characteristics will be selected for more detailed study.

One of the waste streams being considered for "clean-up" of radioisotopes by earth materials is waste water from the MTR. A preliminary resin column experiment was conducted to determine whether specific radioisotopes in this waste were predominantly in the cationic or anionic form. Samples of the influent and effluent streams, and cation and anion resins, were examined by gamma ray spectroscopy over a 78-day decay period. The radioisotopes Ba-140, I-131, and Fe-59 were predominantly on the cation resin; La-140, Zr-Nb-95, Cs-137, and Ce-144 were found on the cation resin only; Co-58 was predominantly on the anion resin. Inasmuch as the earth materials are essentially cation exchangers, the majority of the radioisotopes in the MTR waste should be removable by an ion exchange reaction with earth materials.

*Work performed under a special arrangement with the IDO Health and Safety Division.

V. WASTE CALCINATION DEVELOPMENT AND DEMONSTRATION

(Section Chiefs: R. A. McGuire, Development Operations; K. L. Rohde, Chemistry; J. I. Stevens, Development Engineering; C. M. Slansky, SRI Project Liaison)

Laboratory and pilot plant studies of the fluidized bed calcination process for reduction of high-level wastes to a granular, free-flowing solid have been underway at the ICPP for several years. Early studies were conducted in 3-inch and 6-inch-diameter units; currently, a 12-inch-diameter, electrically heated unit and a 24-inch-square, NaK-heated unit are used for pilot plant studies with non-radioactive material. A 48-inch-diameter Demonstrational Waste Calcining Facility (DWCF) has been built for demonstration of this process with full-level wastes; cold startup testing of the DWCF is underway.

Although exploratory studies have been made to demonstrate the feasibility of the fluidized bed calcination process for stainless-steel and zirconium fuel wastes, the overwhelming majority of the work to date has been concerned with wastes from the processing of uranium-aluminum alloy fuels. A typical waste of this type contains 1.74-molar aluminum nitrate, 0.6-molar nitric acid, 0.01-molar mercuric nitrate, 0.04-molar sodium nitrate, fission products, and other minor components. Studies to date have shown that calcination between 350°C and 550°C, with a superficial fluidizing gas velocity of about 1 ft/sec, produces a suitable product at high throughput rates.

Feed rates up to 120 l/hr have been sustained over long periods of time in the 24-inch-square pilot plant calciner, the capacity apparently being limited by the heat transfer area provided. Volume reduction factors from aqueous waste to bulk stored solids of from 8 to 24 have been demonstrated. A desirable product has been defined as one having a mass median diameter between 0.3 and 0.6 millimeter, a low intra-particle porosity, and a low attrition rate. Particle size has been found to be controllable by variation in the nozzle air-to-liquid ratio, and particle porosity has been found to vary directly with calcination temperature and feed aluminum concentration.

A major problem encountered in these studies has been the elucidation of the factors affecting the rate of conversion of the originally formed, attrition-resistant amorphous form* of alumina to the more friable alpha form. Four variables had been found previously to be of prime importance in this regard: temperature, composition of the gaseous environment, method of alumina formation, and sodium content of the feed solution. Considerable additional information on this problem was gained during the quarter.

Basic studies on the effect of environmental gas composition on formation of alpha alumina were continued. The capability of boric acid, added to the liquid feed to the calciner, to inhibit the formation of alpha alumina was suggested by laboratory studies and was confirmed in two runs in the 24-inch pilot plant calciner and in an extended period of operation of the DWCF.

Other pilot plant studies were conducted to study the off-gas recycle concept (12-inch calciner) and to obtain additional data regarding the sources

* Based on X-ray diffraction measurements.

of overhead fines (24-inch calciner). Additional equipment modifications were made to the DWFC.

1. BASIC STUDIES ON ALPHA ALUMINA FORMATION

1.1 Studies on Effect of Atmospheric Composition (D. W. Rhodes, Problem Leader; R. F. Murray)

Gas composition in the fluidized bed calciners is a dependent variable subject to considerable variation as various independent variables are changed. The effect of such changes on rate of formation of alpha needs to be known and was studied further in a static test unit. Calcined alumina was heated in this unit with fumes of air and nitric acid or of wet or dry oxides of nitrogen. Results of these tests are shown in Table XI.

The results indicate that water vapor in combination with the oxides of nitrogen, NO or NO_2, accelerated the growth of the alpha phase compared to the growth in the dry gases. The wet NO_2 appeared to be more effective than wet NO; however, the relatively wide differences between the alpha content of the two identical control samples (IV-A) suggest that the difference in the effect of the two gases may not be great.

Table XI

EFFECT OF GAS COMPOSITION ON THE GROWTH OF ALPHA ALUMINA

Sample Source		Alpha Alumina Content of Calcine (wt%)					
		Before Heating	After Heating in Given Atmosphere for 24 hr at 400°C				
Pilot Plant Run No.	Hours after Run Startup		HNO_3 + Air	Dry NO	NO + H_2O	Dry NO_2	NO_2 + H_2O
21	100	< 5	54	< 5	19	< 5	53
21	200	< 5	78	< 5	~ 5	< 5	71
21	315	< 5	76	< 5	60	< 5	84
22	65	5	81	< 5	52	< 5	79
22	90	5	58	7	56	8	No sample
22	115	17	40	24	46	20	49
22	150	12	51	15	38	14	54
Control (IV-A)	—	< 5	65	7	57	9	76
Control (IV-A)	—	< 5	76	6	32	8	64

1.2 Basic Studies at Stanford Research Institute (C. M. Slansky, Project Liaison)

Under subcontract, the Stanford Research Institute has supplemented the ICPP studies on factors affecting alpha alumina formation with work directed to the more fundamental aspects of the problem. The first phase of this work was concluded this period, and was made along four lines of endeavor: a search was made for intermediates present during calcination which would give an indication of subsequent crystalline phases; the "structure" of amorphous alumina was studied by examination of X-ray diffraction data; the effect of various additives on the crystallinity of the calcine was studied; and the distribution of crystalline material in individual calcine particles was determined by electron diffraction techniques.

The conclusions of this work are summarized in the following paragraphs [11].

New phases of alumina were found in the course of the research. A-phase, formed at 150 psi at 400°C, had also been found to be formed at 1200 psi from aluminum metal and water. A C-phase was found which may be a dibasic aluminum nitrate (Diban), which was different from the crystalline Diban compounds found at the National Reactor Testing Station. A B-phase was also found, but not in sufficient purity to characterize. These new phases may be important in the transformation of aluminum nitrate to alpha alumina. Structural considerations suggest that amorphous alumina produced in the pilot plant might be structurally related to alpha alumina. Radial distribution analysis of pilot plant samples and synthetic aluminas was studied to determine the structure, but the results were inconclusive. Various factors which contribute to formation of alpha alumina are: (1) sodium acting as a mineralizer or included in the structure, (2) nitrate and water vapor in intermediate compounds or aiding the mobility of the aluminum and oxygen atoms, and (3) conditions unique to fluidization (eg, cycling of temperature and cycling of composition in various zones and rate of decomposition).

Theoretical considerations were applied to the effect of additives on the type of crystal (ie, alpha or gamma alumina), on the size of crystallites, and on amorphous alumina. Formation of alpha alumina might be aided by elements (ie, sodium, calcium) which form structures in which there is hexagonal close-packing of the oxygen atoms. Other additives (eg, zinc), which form spinels with a cubic close-packed arrangement of oxygen atoms, might favor a gamma type of alumina. The prevention of growth of crystallites by strong adsorption of foreign atoms is a possibility. Some additives (eg, boron, phosphorous, and silicon) form strong bonds with aluminum and oxygen atoms but have sizes, coordination numbers, and atomic charges which hinder the growth of continuous regular structure. These are used in glasses and would be likely to favor amorphous alumina.

Electron diffraction examination was made on particles from selected pilot plant samples. Wedge-shaped sections were examined along a diameter to determine where alpha alumina was initially formed. The random distribution of the most intense patterns indicated that alpha alumina formed over fairly large sections of the particles, (not necessarily at the center or edge) and not randomly in small spots distributed throughout the particle. The electron diffraction also showed that amorphous alumina had sufficiently small crystallites to appear amorphous to electron diffraction as well as to X-ray diffraction.

2. SUPPRESSION OF ALPHA ALUMINA BY BORIC ACID

(B. M. Legler, D. W. Rhodes, Problem Leaders;
R. F. Murray, L. T. Lakey, B. P. Brown, P. N. Kelly)

The suggestion from the SRI work that boric acid might suppress the formation of alpha alumina in calcine was followed by a limited laboratory check at the ICPP, and was confirmed by runs in both the pilot plant calciner and the DWCF.

A few tests of the inhibiting effect of boric acid were made in the laboratory by addition of dry boric acid to dry calcine prior to heating in the static test unit. A comparison of the results of these tests with control tests is given in Table XII. It can be seen that boric acid definitely represses the growth of alpha alumina when added to the calcine as the dry solid.

Two runs were made in the 24-inch-square pilot plant calciner to determine the effectiveness of boric acid solution as a feed additive for suppression of alpha alumina formation. Alpha alumina began to appear within 12 hours after startup of run 23-B under conditions defined by a feed composition of 1.29-molar aluminum nitrate, 2.34-molar nitric acid, 0.078-molar sodium nitrate, and 0.015-molar mercuric nitrate; a bed temperature of 400°C; a nozzle air-to-liquid volumetric ratio of 450; and use of a flat-faced stainless-steel nozzle. After 96 hours the alpha alumina content had increased to 51 per cent. Boric acid was then added to the feed at a 0.2-molar concentration and the alpha alumina content of the product decreased to 5 per cent within 84 hours, closely following the calculated "washout" rate. This result strongly indicates suppression of the alpha alumina formation by the presence of boric acid in the feed.

Two boron-containing samples from run 23 were heated in the static test unit under conditions similar to those reported in Table XII. One of these samples, a sample of overhead fines taken 6 hours after introduction of boric acid, changed only from 15 to 22 per cent alpha during heating. The other,

Table XII

EFFECTS OF DRY BORIC ACID ON GROWTH OF ALPHA ALUMINA IN CALCINE

Sample Source		Alpha Alumina Content (wt%)		
		Before Heating	After Heating	
Run No.	Hours after Run Startup		With Boric Acid Addition(a)	Without Boric Acid Addition
PP-23	165	< 5	< 5	47
PP-23	208	28	38	71
DWCF-5	2	5	5	47

Conditions: Temperature, 400°C; heating time, 24 hr; atmosphere, air plus HNO_3 vapors.

(a) 3 wt% boron added as solid boric acid.

a product sample taken 31 hours after introduction of boric acid, changed only from 26 to 31 per cent alpha during heating. These are much smaller changes than are encountered by heating boron-free calcine, thus supporting the premise that boron addition does make the calcine more resistant to conversion to the alpha form.

A second pilot plant test was conducted during run 24 which was carried out under the same conditions as run 23-B, cited above. Boron-free product containing 14 per cent alpha alumina, collected during the first portion of run 23-B, was used as a starting bed. The alpha alumina content of the product increased to a high of 38 per cent during the first 66 hours of operation and then decreased to 21 per cent during the next 36 hours of operation. During the ensuing 47 hours of operation, the alpha alumina content slowly decreased and appeared to stabilize at 15 per cent. Boric acid was then added to the feed at 0.05-molar concentration. The alpha alumina content remained at 15 per cent for 28 hours and then decreased to 6 per cent in the remaining 44 hours to the end of the run. No changes in operating conditions other than addition of boric acid were made during this run. The particle size increased continuously during the period of the boric acid solution, but no attempt was made to control this growth.

A further test of the effectiveness of boric acid in suppressing alpha alumina formation was then made in the DWCF during run 5. On that run, the originally amorphous starting bed converted to 71 per cent alpha alumina during the first 50 hours of operation. At that time, 0.2-molar boric acid was added to the feed, and the alpha alumina concentration began to decrease immediately. By the end of the run 19 days later, the alpha alumina concentration was 8 per cent, the bulk density was 0.94 g/cc, and the mass median particle diameter was 0.5 millimeter and was still increasing.

These results, cumulatively, are very convincing evidence that boric acid as a feed additive is an effective suppressant of the formation of alpha alumina. The mechanism by which boric acid inhibits alpha alumina formation is not yet known, but it is no doubt significant that crystalline sodium nitrate, as indicated by X-ray diffraction, essentially disappeared when boron was present; this suggests a possible reaction between boron and sodium.

Controllability of the particle size of boron-containing calcine, the possibility of caking tendencies, and other side effects remain to be investigated. The minimum effective concentration of boric acid in the feed is another important factor which has not yet been determined.

3. PILOT PLANT DEVELOPMENTS

(B. M. Legler, Problem Leader; L. T. Lakey, B. P. Brown)

3.1 Spray Nozzle Observations

3.11 Effect of Nozzle Design on Alpha Alumina Formation. Use of a boron carbide nozzle, installed in the pilot plant 24-inch calciner to test erosion resistance, appeared to result in a reduced probability of formation of alpha alumina. This effect is possibly related to the different spray characteristics resulting from the much sharper edge on the annular air

orifice in the boron carbide nozzle [3] as compared with the standard flat-faced stainless-steel nozzle.

Evidence of this nozzle effect was found in run 23 in which considerable difficulty was at first encountered in formation of alpha alumina in order to test the effectiveness of boric acid as a control agent. Run 23 was begun using a boron carbide nozzle cap and operating conditions used previously: 400°C bed temperature; 1.0 ft/sec superficial fluidizing velocity; 80 l/hr feed rate; nozzle air-to-liquid volume ratio of 600; and feed containing 1.29-molar aluminum nitrate, 2.34-molar nitric acid, 0.078-molar sodium nitrate, and 0.015-molar mercuric nitrate. The average bed residence time was increased from 25.7 to 33.0 hours (29 per cent) by raising the product overflow level six inches. No detectable alpha alumina was found in the product after 55 hours of operation at 400°C. Continued operation for 77 hours at 500°C, followed by 48 hours at 550°C, likewise failed to produce detectable amounts of alpha alumina. An accidental overheating of the bed to 650°C then melted a flange gasket and forced a shutdown of the calciner, concluding part A of the run. During the shutdown, the boron carbide flat-faced feed nozzle cap was replaced with a stainless-steel flat-faced cap. Part B of run 23 was then conducted at 400°C with a reduced nozzle air-to-liquid volumetric ratio of 450. Within 12 hours after startup, alpha alumina began to appear in the product, as discussed in the preceding section.

The possibility that different feed atomization characteristics of the stainless-steel nozzle cap, as compared with the boron carbide cap, were responsible for creating alpha alumina in part B is clouded by the accidental bed overheating which also may have been a contributing factor.

An additional observation during run 23 as compared with run 22 [3], which also was made using the boron carbide nozzle, was that increased sodium content of the feed (0.25 molar compared with 0.078 molar) did result in alpha alumina formation in run 22, while increases in temperature (from 400°C to 550°C) and residence time (29 per cent) at the lower sodium concentration did not bring about alpha alumina formation.

3.12 Boron Carbide Erosion Resistance. The boron carbide nozzle cap, removed after 738 operating hours, showed no visible evidence of erosion. A retaining flange on the cap broke during removal, thereby eliminating the possibility of weight loss determination. Although boron carbide is the most attrition-resistant of any material tested to date, its inherent brittleness makes its use undesirable unless a change in the cap design can eliminate installation stresses.

3.2 Studies of Particulate Loading

A third run, No. 25, was made in the 24-inch pilot plant calciner during this period to determine the relative effect of nozzle air rate, feed rate, and fluidizing air velocity on off-gas particulate loading. This run was started at the same conditions used in run 24, except that the superficial fluidizing velocity was decreased from 1.0 to 0.5 ft/sec and the boric acid concentration in the feed was increased from 0.05 to 0.10 molar. After 63 hours of operation in which bed fluidization at this low velocity was determined to be adequate, a program of short operating periods at various nozzle air and feed rates was started to study the effect of these variables on the rate of elutriation of the fines from the bed. The data obtained are summarized in Table XIII. A reduction

Table XIII

EFFECT OF VARIABLES ON OFF-GAS PARTICULATE LOADING

Fluidizing Velocity (ft/sec)	Feed Rate (l/hr)	Nozzle Air Rate (cfm)(a)	Average Fines Elutriation Rate(b) (g/hr)
1.0	80	21	1000(c)
0.5	80	21	800
0.5	40	21	250
0.5	40 (H_2O)	21	250
0.5	0	21	30
0.5	0	0	< 10

(a) Measured at calciner pressure and 70°F.

(b) Includes bottoms from primary cyclone plus solids collected in the venturi scrubber.

(c) Measured on Run 24.

of about one-fifth in the fines elutriation rate was obtained by lowering the fluidizing velocity from 1.0 to 0.5 ft/sec. A two-thirds reduction in rate of fines production when the feed rate was lowered from 80 to 40 l/hr indicates that spray characteristics affect the rate of fines production. The extreme reduction in fines production obtained by cutting off the liquid feed makes it apparent that the bulk of the fines is being produced from the fresh feed, either through spray drying or breakoff of the fresh coating from the particle surface. The nearly identical rates observed when using either water or synthetic waste feed indicate that abrasion of the particle coating, rather than spray drying, is the major source of fines.

3.3 Johnston Pump Bearing Test

A Johnston pump equipped with boron carbide sleeves and type 440-C stainless-steel journals was operated 1052 hours on an alumina slurry produced at the DWCF. After disassembly, no measurable wear was found on the boron carbide sleeves, but up to 0.6-mil wear was found on the stainless-steel journals. The bowls of each stage were badly eroded during these tests.

3.4 Off-Gas Recycle Studies

Initial operation was achieved with a new 12-inch pilot plant calciner designed to permit study of fluidization with recycled off-gas, thereby minimizing the net release of off-gas and possible contaminants to the atmosphere. First results indicate that this calciner can be operated under a moderate vacuum (10.75 psia) while using recycled off-gas as the fluidizing medium, as the feed atomizing gas, and as the motivating gas for the dry fines return jet-pump. Analyses of off-gas samples show that essentially all of the nitrogen

oxides are removed in passing through the off-gas condenser and by contact with the off-gas blower seal water. The net off-gas consists essentially of air from instrument purge lines and from in-leakage.

4. DEMONSTRATIONAL WASTE CALCINING FACILITY
(B. M. Legler, Problem Leader)

The DWCF was operated for a total of 30 days this quarter, permitting completion of two runs, 4 and 5. Starting conditions for both runs were a feed rate of 60 gph; a bed temperature of 400°C; an average recycle rate of 20 gph of scrub solution to the feed; a nozzle air-to-liquid volume ratio of 300; and a feed composition simulating the contents of waste hold tank WM-185 (1.74-molar aluminum nitrate, 0.59-molar nitric acid, and 0.039-molar sodium nitrate).

The objective of run 4, started late in the previous reporting period, was to determine the effects of equipment changes and of a sand starting bed on calciner operability and on product properties. In this run alpha alumina reached 45 per cent by the end of the 13-day operating period. The properties of the final product were those typical of a high alpha content material; the final bulk density of the product was 1.62 g/cc and the final mass median particle diameter was 0.23 millimeter. A significant quantity of solids passed through the primary cyclone and contributed to a high concentration of undissolved solids (10 per cent by weight) in the recirculating quench and scrubber solution. This was, however, the first run in which quench solution recycle was possible throughout the entire operating period. The newly installed Lawrence quench pump operated satisfactorily despite the high concentration of undissolved solids in the quench solution. An attempt was made to operate the calciner with the product overflow valve in a fixed position to allow the calciner bed to seek an equilibrium level. However, this method of operation resulted in a bed level so low that the feed nozzles probably were exposed. In the final stages of the operating period, the bed level was maintained well above the feed nozzle location by restricting the product overflow; this seemed to provide more stable operation, but an unscheduled shutdown caused by a helium leak did not allow adequate time for equilibrium operating conditions to be reached. The run was interrupted unexpectedly after eight days of operation when a helium leak developed in a blanket tube in the calciner heat exchanger bundle. A sleeve was welded over the leak and the run was continued an additional five days until another leak developed in the same helium tube. Both leaks occurred in heat-affected zones adjacent to the tube weld. Inspection after the final shutdown revealed no serious caking in the calciner, and the dipleg and primary cyclone appeared to be clear.

The second helium leak was repaired by completely encasing the faulty helium blanket tube in a shroud tube. Additional preparations for the subsequent run included the installation of new caps in the calciner distributor plate (to give a higher pressure drop across the plate), a boron carbide nozzle cap on one of two feed nozzles, and an inspection port in the venturi scrubber inlet gas line.

Operating conditions for run 5 were essentially the same as those for run 4 except that amorphous alumina was used as the starting bed and boric

acid was added to the feed after 50 hours of operation to suppress alpha alumina formation. Two unscheduled shutdowns were made during this run due to plugs in the recirculating off-gas quench system. During each shutdown, the quench solution was replaced by fresh water because of the high undissolved solids concentrations. In an attempt to improve the efficiency of the primary cyclone, the superficial fluidizing velocity was increased from 1.0 to 1.5 ft/sec four days prior to run termination. However, no improvement in the primary cyclone efficiency was apparent.

After shutdown, several lumps of alumina were found in the calciner and large cakes were discovered surrounding the two feed nozzles. The boron carbide-nozzle cap was missing and apparently had fractured and fallen inside the calciner during operation. The stainless-steel cap on the other nozzle was not visibly eroded but did have some solids adhering to its surface. The primary cyclone was plugged with marble-size lumps of calcine of undetermined origin, lying on the directional vanes of the cyclone elements. The dipleg and the lower portion of the primary cyclone contained product particles, which indicates that the calciner bed was being lost through the dipleg just prior to shutdown. The possible relationship of the missing nozzle cap to the unusual solids formation and operating difficulties is apparent; however, a positive tie-in is not possible since the time of failure is not known and insufficient operating experience is available to eliminate the possibility of other sources of trouble.

Six major difficulties have been defined by these two runs and are being studied for possible corrective action prior to the next operating period. These are: (a) excessive solids passing through the primary cyclone with consequent overloading of the quench system; (b) poor control of the feed flow rates; (c) vibration and solids-buildup in the transport air blowers; (d) equipment vent filter plugging; (e) plugging of the solids samplers; and, (f) apparent overstressing of the calciner NaK heat exchanger tubes by the fluidizing action of the bed.

5. POT CALCINATION
(B. R. Wheeler, Problem Leader)

Process flowsheet preparation was completed and detailed design was started for a hot pilot plant installation to demonstrate the Pot Calcination process. Equipment for this demonstration, being conducted in cooperation with the Chemical Technology Division of Oak Ridge National Laboratory, will be installed in cells 1 and 2 of the recently completed Hot Pilot Plant. Preparation of line index drawings, cell layouts, and detailed vessel designs is well underway. A critical path scheduling diagram is being used for planning and expediting on this project.

VI. THE ARCO PROCESS: DISSOLUTION OF FUEL ALLOYS IN MOLTEN CHLORIDE SALTS

(Section Chief, K. L. Rohde, Chemistry)

1. URANIUM DIOXIDE DISSOLUTION

(H. T. Hahn, Problem Leader; E. M. Vander Wall, D. L. Bauer)

A topical report [12] which describes the copper-catalyzed dissolution of uranium dioxide in the chlorine-lead chloride systems has been completed. The conclusions of this investigation are summarized as follows:

(a) An integral dissolution of zirconium-clad uranium dioxide fuels is possible in the lead chloride-cupric chloride system at 550°C. The uranium product is uranyl chloride. In the absence of copper and chlorine, uranium dioxide dissolves at a negligible rate so that zirconium cladding could be removed without any appreciable uranium dissolution.

(b) Stainless-steel-clad uranium dioxide fuels can be dissolved integrally; copper may not be needed, since iron will catalyze uranium dioxide dissolution in the chlorine-lead chloride system.

(c) The uranium dioxide dissolution rate is directly proportional to the cuprous chloride concentration if chlorine is in excess.

(d) The dissolution rate of uranium dioxide can be controlled by three factors in this system: the copper concentration, the chlorine flow, and the surface area.

(e) The active chlorinating agent in the copper-chlorine-lead chloride system is cupric chloride.

(f) The dissolution rate is not strongly temperature-dependent. This makes practical uranium dioxide dissolution rates attainable in chloride systems at 430°C or less.

2. NIOBIUM DISSOLUTION

(H. T. Hahn, Problem Leader; J. L. Teague)

A topical report [13] concerning niobium behavior in the lead chloride and chlorine-lead chloride systems has been completed. The results have shown that:

(a) The rate of dissolution of niobium in lead chloride is quite low but may be increased by stirring. It is believed that the initial reaction is diffusion-controlled; however, a subsequent reaction is linear in rate and possesses an activation energy of 23.4 Kcal/mole.

(b) Volatilization of dissolved niobium from lead chloride is principally due to the presence of niobium pentachloride; the presence of lower oxidation states of niobium leads to incomplete volatilization. Niobium trichloride

was tentatively identified in the sublimate, and insoluble niobium (IV) oxide was found in aqueous extracts of the melt.

(c) The rate of dissolution of niobium in chlorine-lead chloride melts is feasible for process application at reasonable temperatures, eg, 12 mg min^{-1} cm^{-2} at 550°C and 120 mg min^{-1} of chlorine, Volatilization of niobium pentachloride from the chlorinated melt is 99.9 per cent complete at 550°C.

VII. BASIC PROCESS STUDIES AND EQUIPMENT DEVELOPMENT

(Section Chiefs: R. A. McGuire, Development Operations;
K. L. Rohde, Chemistry; J. I. Stevens, Development Engineering)

1. EXPERIMENTAL AIR PULSER

(E. E. Erickson, Problem Leader; S. J. Horn,
with assistance of the AED Instrument Development Branch)

Air pulsers were designed and installed on the plant columns, and have operated very successfully. However, no adequate means is available to measure pulse amplitude directly. Continuing work on air pulsers is directed toward developing instrumentation to measure and control pulse amplitude, achieving a better understanding of hydraulic behavior of pulsed systems, and simplifying air pulser design equations.

To this end, an experimental air pulser and column have been set up. Most of the deficiencies in the instrumentation associated with the experimental air pulser have been corrected, and an initial group of runs is being made to check out the entire system. The instrumentation which has required the most development work is that which is associated with the measurement of flow rates and the air-liquid interface position. Some uncertainty, particularly at the higher frequencies and amplitudes, was associated with visual measurement of the position of the moving interface within the glass pulser leg. It was hoped that integration of the flow measurements with respect to time would yield more reliable data.

Figure 8 is a block diagram of the circuitry used to indicate flow and interface position.

The Ramapo flow transducer installed in the pulser leg provides a millivolt level signal which is proportional to the square of the volumetric flow rate of the fluid in the pulser leg. The Sanborn model 350-1500 dc strain gage preamplifier is part of the data recording system and includes the necessary excitation voltage, bridge balance, and calibration controls for the flow transducer. It also provides an output voltage which is a voltage analog of the transducer output as recorded, and therefore is influenced by the attenuator setting on the preamplifier. This output voltage is the input to a 3-stage computer using standard dc operational amplifiers. The first stage is a voltage amplifier, the second stage extracts the square root of the amplified voltage to provide

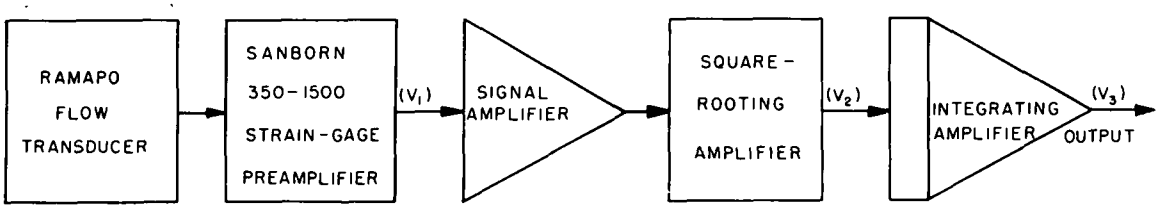

CPP-S-2143

Fig. 8 Block diagram of flow and position computer.

a signal proportional to the velocity, and the third integrates the velocity signal to represent the position of the fluid in the pulse leg.

The instrument was calibrated by comparing the output of the integrator with the interface position observed in the glass pulser leg. The calibration runs were made at either a low frequency or a low amplitude in order to minimize the uncertainty in the visual observations.

The results of the calibration runs, summarized in Table XIV, show reasonably good agreement (within 5 per cent) on pulse amplitude. Some electronic problems associated with the integrator were experienced between runs 3 and 4, which may explain why the indicated values were greater than measured values in runs 1 to 3 and vice versa in runs 4 to 7.

The experimental air-pulsed column has been studied by simulation on the analog computer using the same methods that were used to simulate plant extraction columns [3, 7, 14]. The frequency and amplitude of the runs completed to date were chosen for calibration purposes, and only two can be compared with the analog simulation. The amplitudes from these two computer runs are given in Table XIV. The values from analog simulation are within 2 to 3 per cent of the two comparable runs on the experimental column.

Table XIV

CALIBRATION RESULTS FOR EXPERIMENTAL PULSE COLUMN (a)

Run No.	Frequency (cycles/min)	Reservoir Pressure (psig)	Mean Operating Position (in.) (b)		Pulse Amplitude (in.)		
			Indicated	Measured	Indicated	Measured	Analog Simulation
1	19.5	4.6	71.2	62.4	63.9	61.3	—
2	19.5	5.8	79.8	77.6	76.7	72.8	—
3	14.7	5.4	73.6	76.3	108	107.5	—
4	14.6	5.8	75.4	80.1	105	108.8	—
5	14.6	4.4	59.6	60.3	87.3	92.0	—
6	25.1	4.4	56.9	58.0	36.1	36.5	35.2
7	34.2	4.4	60.5	63.4	18.8	19.3	18.9

(a) Operated with water.
(b) Average difference in hydraulic head between column overflow and pulse leg.

2. PULSE COLUMN DYNAMICS

(E. E. Erickson, Problem Leader; E. L. Rowe)

A study of pulse column dynamics has been undertaken in order to specify and evaluate column control requirements. Some results of this work were reported previously [7]. The equations simulating pulse column behavior required assumptions on individual phase holdup within the column. Work is continuing to determine phase holdup as well as phase composition in an experimental column to insure the adequacy of the mathematical model.

The phase-separating capabilities of porous stainless steel and plastics were evaluated for possible pulse column sampling means. Under appropriate conditions, D, E, and F grades of porous stainless steel passed only water from a finely dispersed equal-volume mixture of hexone in water. Porous Kel-F and porous Teflon, 1/16 inch thick, passed only hexone. The D grade stainless steel transmitted water at an initial flow rate of 0.29 ml/(cm^2)(sec), with a pressure difference of 2 inches of water. The porous Kel-F gave an initial flow rate of 0.19 ml/(cm^2)(sec) of hexone under the same conditions. The other materials tested had smaller pore sizes and gave much lower flow rates at comparable pressure difference.

A segmented Pyrex pulse column, 1-1/2 inches ID, has been installed in the laboratory for experimental studies. Pulse and step transients for feed composition and flow can be introduced from auxiliary feed supply tanks and pumps by appropriate positioning of solenoid valves. The system is undergoing some modification in order to attain proper operation of positive displacement, high frequency, metering pumps, and the necessary calibrations are being made.

3. EVAPORATOR CONTROL

(E. E. Erickson, Problem Leader; L. A. Jobe)

Final adjustments of the cascade control system for the first cycle product evaporator (H-130) were based on tests made after installation in the plant [3]. The steam to the evaporator is controlled by a flow recorder-controller on the evaporator feed, with the set point for this controller in turn regulated by a density recorder-controller. The frequency response characteristics of the density recorder-controller, determined by means of a pneumatic sine-wave generator having a range of 0.0004 to 60 cpm, showed that the controller did not have a built-in limitation to restrict the maximum phase lag of the reset action. Thus, the full 90° phase lag at low frequencies had to be considered in adjusting the H-130 control system. Since the reset time setting is critical for stability, and since pneumatic controller settings have been reported as being up to 100 per cent in error, the reset action was calibrated for this controller. The results showed the values marked on the controller to be reasonably accurate.

An experimentally determined transient curve for the evaporator, shown in Figure 9, was found to be remarkably similar to that for a first order system. Using the effective time constant of 70 minutes determined from the curve, instrument settings and an allowable reset time were calculated. The settings were 200 per cent proportional band on the flow actuated controller, and 80 per cent proportional band with 10 minutes reset time on the density controller. After the plant was brought on stream and the effects of normal plant upsets upon the controlled density were

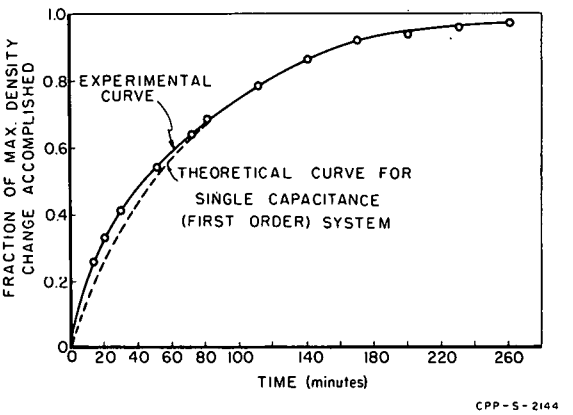

Fig. 9 Transient test curve for H-130 evaporator.

observed, minor changes in controller settings were made to increase controller response short of instability. The final settings were: 170 per cent proportional band and 100 per cent pneumatic-set span on the flow actuated controller; and 100 per cent proportional band and 20 minutes reset time on the density controller. The close agreement between the two sets of figures demonstrates the value of the theoretical approach to controller settings.

The control of the evaporator has been very successful for relatively large, sharp variations, as well as for periodic oscillations of ± 15 to 22 per cent from the mean flow rate, in evaporator feed rates. As an example, major upsets of from -80 per cent to + 15 per cent of the mean flow value, occurring three or four times over a period of 10 minutes, were held to a single density flunctuation of + 10 per cent for a period of less than two minutes, as shown in Figures 10 and 11.

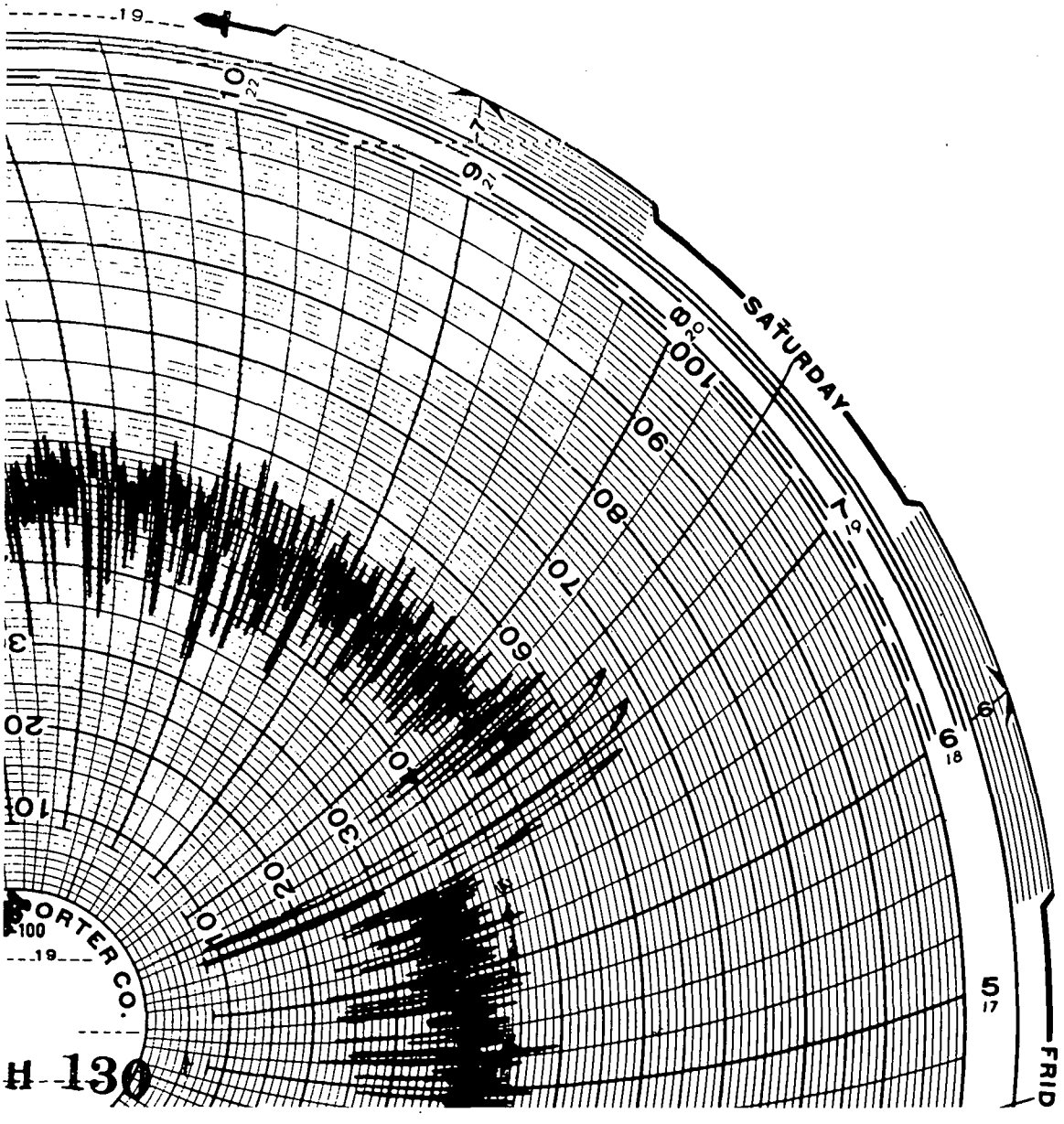

Fig. 10 Feed flow to the H-130 evaporator showing extreme variations in rate (100% chart = 2 gpm).

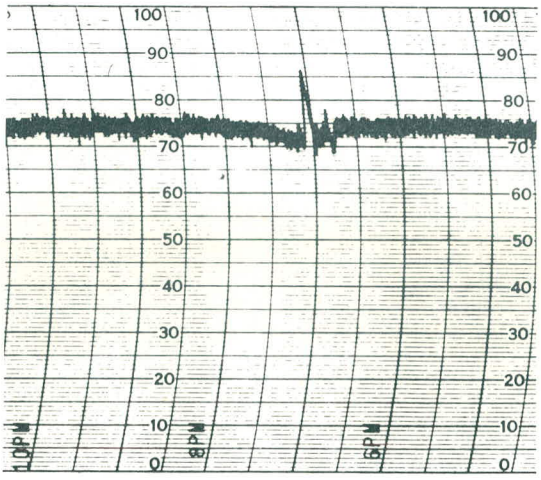

Fig. 11 H-130 record of product density (corresponding to evaporator feed rates shown in Figure 10).

4. REMOVAL OF TRIBUTYL PHOSPHATE FROM DILUTE AQUEOUS STREAMS

4.1 Dibutyl Phosphate Chemistry (H. T. Hahn, Problem Leader; E. M. Vander Wall, D. L. Bauer)

The primary decomposition product of tributyl phosphate (TBP) is dibutyl phosphoric acid. The disposition of dibutyl phosphoric acid between various aqueous and organic plant streams has considerable significance, since it is known to affect extraction performance and may impair the function of moving parts of equipment. Of immediate interest is the behavior of uranyl dibutyl phosphate complexes under conditions in which uranium is stripped from the organic phase and TBP is stripped from the resultant aqueous phase.

The solubility ratios of uranyl dibutyl phosphate between organic phases composed of TBP and Amsco 125-90 W, and an aqueous phase of dilute nitric acid were determined for various concentrations of TBP and nitric acid. It was found that, at low concentrations of nitric acid and TBP, uranyl dibutyl phosphate preferred the aqueous to the organic phase.

The partition of uranium between TBP-Amsco and dilute nitric acid was studied by use of uranium-233 tracer as the concentrations of dibutyl phosphoric acid and TBP were varied. The extraction of uranium by dibutyl phosphate into the organic phase is independent of the concentration of TBP in the organic phase as long as the stoichiometric ratio of dibutyl phosphate to uranium is less than two. In this region, the uranium prefers the aqueous phase. When more than two molecules of dibutyl phosphate are available per atom of uranium, the uranium strongly favors the organic phase.

4.2 Distribution of Uranyl Dibutyl Phosphate Between Tributyl Phosphate-Amsco Solutions and Dilute Nitric Acid Solutions

This phase of the study is of interest in relation to the distribution to be anticipated in the first cycle stripping column where uranium is transferred from the TBP-Amsco solution to dilute aqueous nitric acid solution.

Uranyl dibutyl phosphate was prepared by the slow addition of a uranyl nitrate solution to an aqueous solution of dibutyl phosphoric acid. Identity of the product was confirmed by elemental analysis and thermal decomposition data.

The distribution ratios of uranium were determined as a function of both TBP and nitric acid concentration. The concentration of TBP in Amsco 125-90W ranged from 1.02 to 30.09 weight per cent, while the concentration of nitric acid was fixed at three levels: 0.04, 0.52, and 1.05 molar. Since the concentration of uranium was usually less in the aqueous than in the organic phase, the aqueous-to-organic volume ratio was 20 to 10 milliliters. These

phases were equilibrated for four to five days at 24 ± 2°C with an excess of solid uranyl dibutyl phosphate. The equilibrations were conducted in the dark to minimize any photodecomposition of TBP in the presence of uranium. The solubilities determined in these experiments are presented in Figures 12, 13, and 14. The solubility ratios, based on the concentration of uranium, are plotted as a function of the concentration of TBP in Figure 15.

The data indicate that the solubility ratio of uranyl dibutyl phosphate is dependent on the concentration of TBP in the organic phase; in fact, if the

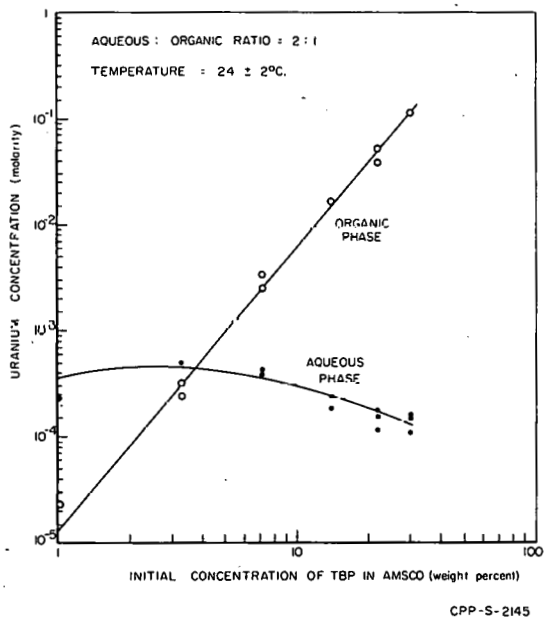

Fig. 12 Solubility of uranyl dibutyl phosphate in tributyl phosphate-Amsco and 0.040M nitric acid solutions at equilibrium.

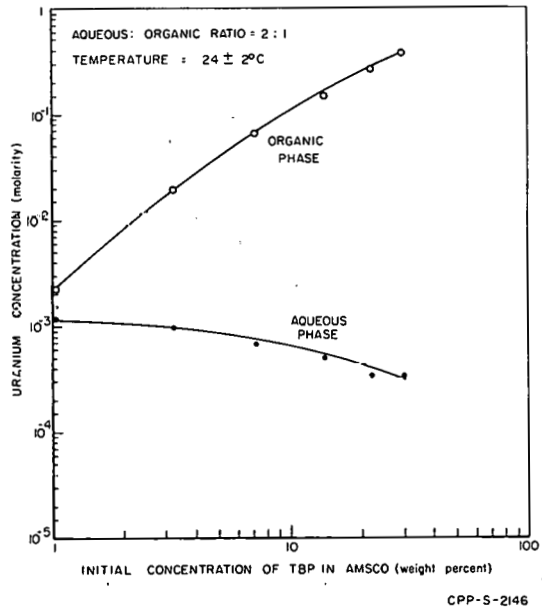

Fig. 13 Solubility of uranyl dibutyl phosphate in tributyl phosphate-Amsco and 0.525M nitric acid solutions at equilibrium.

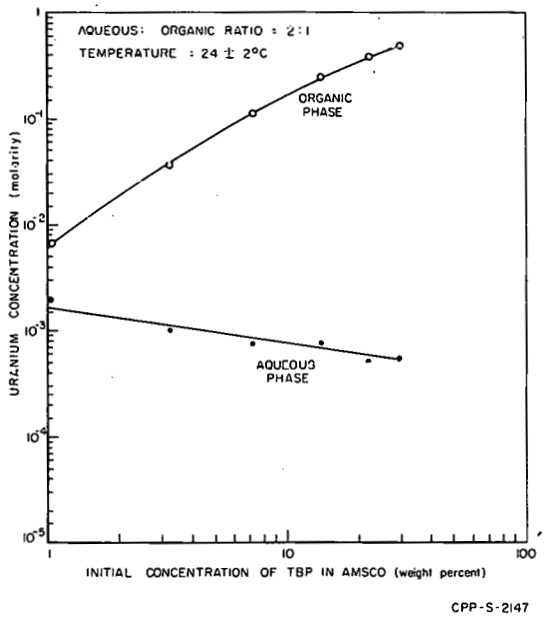

Fig. 14 Solubility of uranyl dibutyl phosphate in tributyl phosphate-Amsco and 1.05M nitric acid solutions at equilibrium.

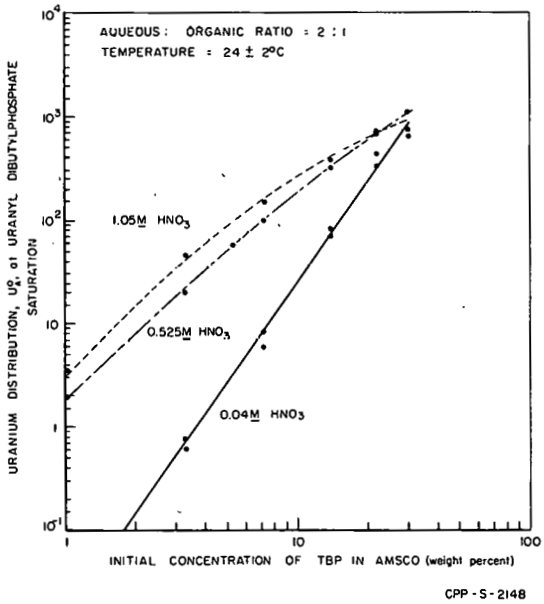

Fig. 15 Solubility ratios of uranyl dibutyl phosphate in tributyl phosphate-Amsco and dilute nitric acid solutions.

aqueous phase is initially 0.04-molar nitric acid, the solubility ratio is proportional to the third power of the concentration of TBP. As the acidity of the initial aqueous phase is increased, the effect of the concentration of TBP on the solubility ratio decreases; but even with 1.05-molar nitric acid in the aqueous phase, the ratio is still dependent to a greater degree than first order on the concentration of TBP. Increasing nitric acid concentration increases the solubility of uranyl dibutyl phosphate in both the aqueous and organic phases. Increasing the concentration of TBP in the system increases the solubility of uranyl dibutyl phosphate in the organic phase, but causes a decrease in solubility in the aqueous phase. The net result is that, at low concentrations of both nitric acid and TBP, uranyl dibutyl phosphate prefers the aqueous phase to the organic phase.

It was noted that in the series of experiments with initial 0.04-molar nitric acid in the aqueous phase, the uranium solubility ratios depended on the third power of the concentration of TBP. Since the aqueous uranium concentration was essentially independent of TBP concentration, it would seem reasonable to assume that three TBP molecules were associated with each uranyl dibutyl phosphate molecule. Formation constants were calculated for such a complex, and the average value with its standard deviation was $(13.2 \pm 6.2) \times 10^2$ as the concentration of TBP ranged from 0.094 to 0.660 molar. Since no straight line relationship occurred in the experiments in which other concentrations of nitric acid were used, no similar constants for other possible complexes were obtained.

4.3 Partition of Uranium Between Tributyl Phosphate-Amsco Solutions and Dilute Nitric Acid Solutions as a Function of the Concentration of Dibutyl Phosphoric Acid

This phase is of concern in the uranium recovery flowsheet which provides for removal of residual TBP from the aqueous product stream by countercurrent washing with pure Amsco.

A simulated stripping column solution was prepared which was 0.02-molar uranium and 0.04-molar nitric acid. This solution contained approximately 5 milligrams of uranium-233 per 250 milliliters and resulted in a specific alpha activity of approximately 5×10^5 disintegrations per minute per milliliter. The Amsco used in these experiments was washed several times with sulfuric acid and then washed repeatedly with distilled water until all the acid was removed. The TBP was vacuum distilled from calcium oxide. The dibutyl phosphoric acid used was at least 99 per cent pure as determined by titration with base. Chemical analysis showed it to contain 14.9 per cent phosphorus compared to the theoretical value of 14.7 per cent phosphorus.

The extractions were performed in the following manner: The desired amount of dibutyl phosphoric acid was weighed directly into a 15-milliliter centrifuge tube either as the pure compound or as a solution of known concentration. Five milliliters of the desired TBP-Amsco solution were then added, followed by five milliliters of the aqueous solution. The solutions were stirred rapidly for four minutes and were sampled from each phase for alpha counting.

The data obtained from these experiments are plotted in Figure 16. The base lines were determined by equilibrating the aqueous stock solutions with

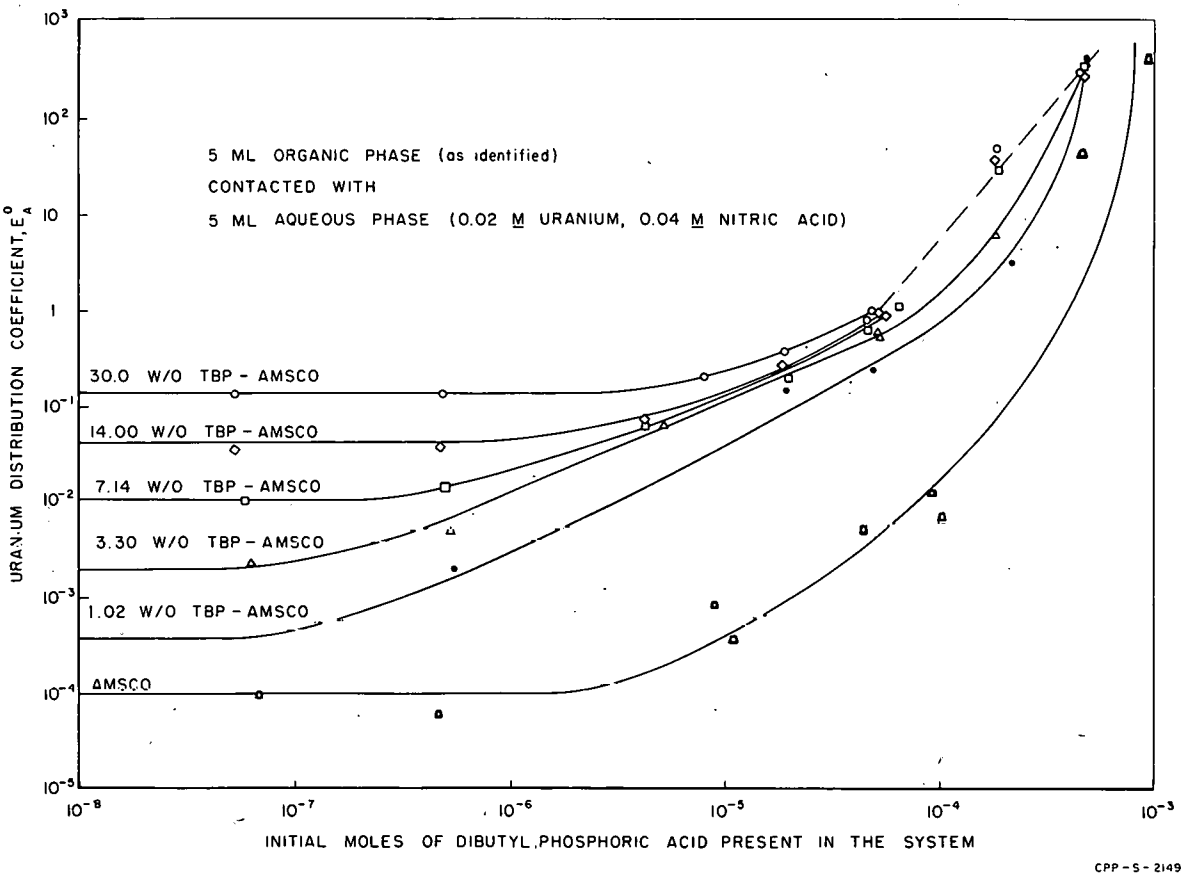

Fig. 16 The distribution of uranium between tributyl phosphate-Amsco and 0.04M nitric acid solutions in the presence of dibutyl phosphoric acid.

the desired solutions of TBP and Amsco in the absence of dibutyl phosphate. A distribution curve for uranium between the aqueous solution and Amsco alone was also obtained as a function of the concentration of dibutyl phosphate.

In the region where the ratio of total moles of dibutyl phosphate to the total moles of uranium is less than one, the uranium appears to be extracted into the organic phase as a complex which contains only one molecule of dibutyl phosphate per atom of uranium. The amount of this complex which extracts appears to be independent of the concentration of TBP but requires the presence of TBP for extraction. As the stoichiometric ratio of total dibutyl phosphate to total uranium varies from one to two, some solid uranyl dibutyl phosphate forms in the system; above a stoichiometry of two, and in all experiments which contained 3.3 weight per cent or a greater concentration of TBP in Amsco, no solids remained after equilibration, indicating that a third complex is formed. At the lowest concentration of TBP used in these experiments (1.02 weight per cent or 0.029 molar), solids continued to remain as the stoichiometry of total dibutyl phosphate to uranium increased from one to five. Therefore, it seems possible that a certain minimum amount of TBP is necessary to form the third complex. Additional experiments are being conducted to establish formation constants, nitrate dependency, and the effect of hydrogen ion concentration on the system.

5. CONTINUOUS RECIRCULATING DISSOLVER

(M. E. Weech, R. A. McGuire)

Previous laboratory data on a small scale recirculating dissolver [15] indicated that greatly improved aluminum dissolution rates could be attained by recirculating solution rapidly through the dissolver. Dissolution is increased, presumably by rapid removal of the gas film that blankets the dissolving surfaces. If recirculation could be applied successfully to the CPM dissolvers, they should give higher dissolution rates at present flowsheet catalyst concentrations or maintain present rates at greatly reduced catalyst concentrations; at the same time, the consistency of the dissolver product should be improved.

Preliminary runs in a newly installed pilot plant recirculating dissolver gave such rapid dissolution, whether recirculated or not, that acid deficient product resulted; the catalyst concentration of 0.005 to 0.003-molar mercury will be reduced in future runs to obtain comparative dissolution rate data. Possible effect of recirculation was noted, however, in that the solution mercury content of the trial recirculating runs was less than half that of the non-recirculated runs, although the mercury concentration in the feed was the same for both type runs. This indicates that the aluminum surface amalgamates to a much greater extent under recirculating conditions than for static conditions; thus, the effective dissolution surface area should be much greater under recirculating conditions. It was found that the mercury in solution was present largely as mercurous rather than mercuric ion.

VIII. REPORTS AND PUBLICATIONS ISSUED DURING THE QUARTER

1. IDO REPORTS ISSUED

IDO-14563, Series Electrolytic Dissolver for Nuclear Fuels I. Scoping Studies, by M. R. Bomar.

IDO-14565, The Dissolution of Iron and Nickel in Dilute Aqua Regia, by A. D. Cannon.

IDO-14566, Containment of Iodine-131 Released by the RaLa Process, by G. K. Cederberg and D. K. MacQueen.

IDO-14569, Pilot Plant Development Studies of a Continuous Process for Recovering Uranium from Nichrome Fuels, by H. V. Chamberlain.

IDO-14571, Electrolytic Oxidation of Zirconium in Nitrate Solution, by M. R. Bomar.

IDO-14575, Electrolytic Dissolution of Nichrome in Nitrate Solutions, by J. R. Aylward and E. M. Whitener.

2. JOURNAL PUBLICATIONS

C. M. Slansky, "Preparation of Fuels for Processing," Chapter III, Chemical Processing of Reactor Fuels, Academic Press, 1961, J. Flagg, Editor.

IX. REFERENCES

1. J. R. Bower, Ed., Idaho Chemical Processing Plant Technical Progress Report, 4th Qtr 1959, IDO-14512, (1960).

2. J. R. Bower, Ed., Chemical Processing Technology Quarterly Progress Report, 1st Qtr 1961, IDO-14560, (1961).

3. J. R. Bower, Ed., Chemical Processing Technology Quarterly Progress Report, 3rd Qtr 1961, IDO-14574, (1961).

4. O. W. Parrett, Modifications for the STR Fuel Recovery Process, IDO-14522, (December 1, 1960).

5. J. R. Bower, Ed., Chemical Processing Technology Quarterly Progress Report, 3rd Qtr 1961, IDO-14574, p 4, (1961).

6. A. G. Chapman and R. A. Woodriff, Zirconium Fluoride Phase Studies, I. A Preliminary Investigation of Solid Phase, IDO-14469, (1959).

7. J. R. Bower, Ed., Chemical Processing Technology Quarterly Progress Report, 2nd Qtr 1961, IDO-14567, (1961).

8. J. R. Aylward and E. M. Whitener, Electrolytic Dissolution of Nuclear Fuels. Part II. Nichrome in Nitrate Solutions, IDO-14575, (December 29, 1961).

9. J. R. Aylward et al, Electrolytic Dissolution of Nuclear Fuels. Part I. Zirconium in HCl Methanol, IDO-14573, (December 29, 1961).

10. M. R. Bomar, Series Electrolytic Dissolver for Nuclear Fuels. I. Scoping Studies, IDO-14563, (November 15, 1961).

11. H. J. Eding et al, Phase Transformations in Alumina, IDO-14580, (February 14, 1962).

12. E. M. Vander Wall et al, Salt Phase Chlorination of Reactor Fuels. III. Catalyzed Dissolution of Uranium Dioxide in Lead Chloride-Chlorine Systems, IDO-14578, (February 5, 1962).

13. J. L. Teague et al, Salt Phase Chlorination of Reactor Fuels. Part IV. Niobium Behavior in the Lead Chloride and Chlorine-Lead Chloride Systems, IDO-14579, (March 15, 1962).

14. M. E. Weech et al, Interim Report on the Development of an Air Pulser for Pulse Column Application, IDO-14599, (September 22, 1961).

15. E. E. Erickson, A Bench Scale Natural-Recirculation Dissolver, IDO-14572, (January 10, 1962).

PHILLIPS
PETROLEUM
COMPANY

ATOMIC ENERGY DIVISION